Copper – Titanium – Zirconium

Tamara Velikanova, Mikhail Turchanin

Introduction

The investigation of the partial isothermal section at 750°C in the Ti rich corner of the system by [1960Bun, 1961Enc] was the first work undertaken on the Cu-Ti-Zr ternary system. The interest in the system was related to the development of a new class of Ti based alloys, which exhibit high strength at elevated temperatures. A number of experimental works [1983Dut, 1988Woy, 1990Che, 1992Kov] on the phase relations in the ternary Cu-Ti-Zr system were stimulated by the discovery of glass formation through rapid quenching of liquid alloys, over a wide concentration range. [1983Dut] reported preliminary results on the liquidus surface in the central portion of the phase diagram. [1988Woy] carried out a more detailed investigation of the system in the range 30 to 100 at.% Cu. A partial liquidus surface and isothermal section at 703°C were presented. The existence of a ternary compound reported previously by [1965Tes, 1969Tes] was confirmed in this work as well as in the investigation of the ZrCu-TiCu section by [1992Kov]. As-cast, annealed and rapidly quenched alloys along the Zr_2Cu-Ti_2Cu section were studied by [1990Che]. The temperature-composition section and the diagram of metastable crystallization of amorphous alloys at 33 at.% Cu were presented. The experimental works devoted to the study of phase relations in the Cu-Ti-Zr system are summarized in Table 1.
A thermodynamic assessment of the system was made by [2003Arr]. The calculation results agreed well enough with the experimental data available, except for some regions in the ternary isothermal section at 703°C. The optimized and self-consistent thermodynamic description of the Cu-Ti-Zr system by [2003Arr] was used in the present assessment for the generation of the majority of phase diagrams. Some figures were corrected because of differences with respect to the accepted Cu-Ti binary system (see Binary Systems and other sections below).

Binary Systems

The Cu-Zr and Ti-Zr systems are accepted from the thermodynamic assessments of [1994Zen] and [1994Kum], respectively. These diagrams are generally consistent with [2006Sem, Mas2]. Reactions associated with the high-temperature $Zr_{13}Cu_{24}$ phase from [1986Kne] as well as the polymorphism of Zr_2Cu described by [2006Sem] are not taken into account in this assessment as there is no consensus of opinion concerning the reliability of the information. The Cu-Ti diagram is accepted from [1996Kum], but with corrections to the Ti rich part. The congruent melting of Ti_2Cu is accepted from [2002Ans], and the nature of the reaction between β, γ and liquid is accepted as eutectic rather than peritectic, as given in [1996Kum].
In [1988Woy], the binary phase diagram of the Cu-Ti system was taken from [1983Mur], and for the Cu-Zr system from [1979Dri]. According to the latter work, the ZrCu phase remains stable at low temperatures. This peculiarity should be taken into account when considering the results of [1988Woy].

Solid Phases

The crystallographic data of the solid phases of the Cu-Ti-Zr system and their temperature and concentration ranges of stability are listed in Table 2.
[1961Enc] found that the solubility of Cu in (αTi) diminishes with the addition of Zr. In agreement with this work, a decrease in the solubility of copper in (αTi) with increasing Zr concentration, as well as a decrease in the solubility of copper in (αZr) with increasing Ti content is shown by the thermodynamic computation of [2003Arr]. The maximum content of copper in the β solid solution in the ternary system is not more than 12 at.%. The extension of the β phase in the ternary system in equilibrium with the α and γ phases (enriched by Ti) is less than ~6 at.% Cu at 750°C. The solubility of Zr in the (Ti,Cu) solid solution is less than 0.01 at.%, as was shown by the calculation of [1961Enc].

The formation of a continuous solid solution (γ phase) between the isostructural binary compounds, Zr_2Cu and Ti_2Cu, was established by [1990Che] for temperatures below 800°C. The lattice parameters of the γ solid solution increase linearly from Ti_2Cu to Zr_2Cu, while the *c/a* ratio decreases [1990Che], as shown in Fig. 1. Previously, the possibility of the dissolution of zirconium in Ti_2Cu at 750°C was remarked by [1961Enc]. Analysis of the thermodynamic model for the γ phase presented by [2003Arr] predicts a miscibility gap with a critical point at 612°C.

The existence of extremely narrow two-phase regions, Zr_3Cu_8 + $TiCu_4$, Zr_3Cu_8 + $Zr_{14}Cu_{51}$, Zr_3Cu_8 + Zr_7Cu_{10}, Zr_3Cu_8 + Ti_2Cu_3 (in the Cu rich region) and Zr_7Cu_{10} + Ti_3Cu_4, Ti_3Cu_4 + τ_1, TiCu + Ti_3Cu_4, ZrCu + τ_1 (in the central portion of the phase diagram) allows one to suppose rather limited homogeneity ranges for the binary phases in the ternary system, not exceeding 5 at.% [1988Woy]. The TiCu and Zr_7Cu_{10} phases, however, dissolve up to nearly 10 at.% of the third component at 703°C [1988Woy]. A solubility of 4 at.% Zr in TiCu at 842°C was reported by [1992Kov].

The ternary τ_1 phase having the Laves type $MgZn_2$ structure was first reported by [1965Tes]. Its composition, reported by [1965Tes, 1969Tes] as $ZrTiCu_4$, was later revised by [1988Woy, 1992Kov] and an average stoichiometry of $ZrTiCu_2$ was proposed. This phase was confirmed in the as-cast and annealed (at 703°C) alloys by [1988Woy]. At 703°C, the extension of the homogeneity range of τ_1 is 25 to 30 at.% Zr and 45 to 50 at.% Cu. According to [1992Kov], at 50 at.% Cu the homogeneity range is 21 to 37 at.% Zr at ~830°C and 22.5 to 29 at.% Zr at 630°C. The phase was established by [1988Woy, 1992Kov] to melt congruently. A melting temperature 867°C at 25 at.% Zr was found by [1992Kov]. From the thermodynamic calculation, the melting temperature is given as 883°C, which is in good agreement with experiment. This phase was observed as a metastable phase in as-cast and melt-spun alloys with compositions along the Zr_2Cu-Ti_2Cu section having Zr contents between 27 and 36 at.% Zr. It transformed into the γ phase under annealing at 700°C.

Thorough experimental investigation of the solubility ranges of ternary τ_1 phase, the binary phases as well as their stability in the ternary system, is needed. It is worth noting that only the α, β and γ phases were treated as ternary solid solution phases in the thermodynamic assessment of [2003Arr].

Quasibinary Systems

It would have been assumed that quasibinary systems exist in the ternary system because quasibinary eutectics formed between the congruently melting compounds have been reported. Quasibinary eutectic maxima were reported to exist by [1988Woy] on the congruent monovariant liquid lines of joint crystallization of the τ_1 phase and ZrCu, Zr_2Cu as well as the TiCu phase. However, the maximum point on the monovariant line corresponding to the L ⇌ τ_1 + TiCu eutectic equilibrium was not confirmed by calculation. At the same time, the ZrCu-τ_1 section was shown to be quasibinary of eutectic type above the temperature of the ZrCu eutectoid decomposition, as shown in Fig. 2. Below this temperature, the three-phase Zr_7Cu_{10} + τ_1 + γ field exists in the section. So the section ZrCu-τ_1 can be considered as only partially quasibinary. The eutectic composition, 50Cu-9.5Ti-40.5Zr (at.%), and a eutectic temperature of 841°C calculated by [2003Arr] are in good agreement with the experimental solidus and liquidus points for alloys along the ZrCu-TiCu section in the composition range 30 to 50 at.% Zr, obtained by [1992Kov]. Additionally, both the τ_1 and TiCu phases form quasibinary eutectics with the highly stable congruently melting $Zr_{14}Cu_{51}$ compound. The calculated τ_1-$Zr_{14}Cu_{51}$ and TiCu-$Zr_{14}Cu_{51}$ sections are shown to be quasibinary systems (Figs. 3 and 4, respectively). For the τ_1-$Zr_{14}Cu_{51}$ system, the eutectic composition and temperature are 55.0Cu-20.7Ti-24.3Zr (at.%) and 879°C. For the TiCu-$Zr_{14}Cu_{51}$ system, they are 61.4Cu-30.4Ti-8.2Zr (at.%) and 885°C. The latter is only 3°C higher than the solidus temperature of the adjoining TiCu + $Zr_{14}Cu_{51}$ + Ti_3Cu_4 three-phase field.

Invariant Equilibria

Tables 3 and 4 list the invariant reactions for the ternary system, taken mostly from the thermodynamic calculation of [2003Arr]. For the thermodynamic assessment of the ternary system, datasets for the binary systems were taken from [1994Kum, 1994Zen, 1996Kum]. In the calculation, all of the solid phases, except for α, β and γ, were considered to be stoichiometric. The reaction scheme in Fig. 5 shows an incongruent

three-phase invariant equilibrium l + β ⇌ γ at 1005°C, calculated by [1996Kum]. This is changed to a congruent reaction l ⇌ β + γ at the same temperature in order to agree with the accepted Cu-Ti binary phase diagram. Agreement was obtained between the calculated temperatures and the data reported by [1988Woy] for the central part of the ternary system. Two invariant equilibria in reaction scheme, E_4 and E_5, out of the three proposed by [1988Woy] were confirmed. The eutectic reactions involving the τ_1 phase were determined by [1988Woy] using the Transient Liquid Phase (TLP) bonding technique. In this procedure, two phases, A and B, differing in composition are brought into contact and assembled into a sandwich structure, such as A/B/A or B/A/B, at a temperature higher than the transformation temperature involving these phases. If a eutectic reaction between them takes place, inter-diffusional processes eventually lead to the formation of a liquid layer at the interfaces. Eutectic regions were identified in the quenched microstructure and the composition of the liquid at the eutectic point was determined using EMPA. Diffusion couples involving τ_1 and either Zr_7Cu_{10}, Zr_2Cu, ZrCu or TiCu were used. The sandwich structures were held at temperatures of around 867°C for 30 min. From these experiments, the three ternary eutectic reactions involving the τ_1 phase were determined: L ⇌ τ_1 + ZrCu + Zr_2Cu (E_4), L ⇌ τ_1 + β + Zr_2Cu (E_5) and L ⇌ τ_1 + Ti_2Cu + TiCu. The temperature of the L ⇌ τ_1 + Ti_2Cu + TiCu reaction was reported by [1992Kov] to be 842°C. This reaction was not confirmed by calculation. Instead, two invariant equilibria with compositions very close to those of the invariant liquid phases and their temperatures, U_4 and E_1, at 856 and 855°C, respectively, were found.

Two degenerated invariant equilibria, D_1 and D_2, including the $TiCu_2$ phase were obtained by recalculation in the current assessment, instead of the P and U types found by [2003Arr]. The degeneracy is caused neglecting the possible Zr solubility in the Cu-Ti binary phases participating in the equilibria. Additionally, a ternary eutectoid reaction ZrCu ⇌ τ_1 + γ + Zr_7Cu_{10} at 720°C (E_6) and transition type reaction $TiCu_4$ + $Zr_{14}Cu_{51}$ ⇌ $ZrCu_5$ + Ti_2Cu_3 (U_9) between 703 and 750°C are proposed based on the preceding monovariant equilibria and comparison of the phase equilibria at 703 and 750°C.

Liquidus and Solidus Surfaces

The liquidus projection, given in Fig. 6a for the whole concentration range of the Cu-Ti-Zr system, as well as an enlarged portion in the Cu rich part of the diagram, Fig. 6b, were recalculated using the thermodynamic data set of [2003Arr]. In Figs. 6a, 6b the substitution of incongruent point p (accepted by [2003Arr]) by congruent e_1 at 30 at.% Cu for l ⇌ β + γ equilibrium is shown. The results of the calculation of the monovariant and of the invariant transformation temperatures are in satisfactory agreement with the experimental partial liquidus projection for the central part of the system reported by [1988Woy], except for some details. For example, the proposed compositions of the temperature maxima of the quasibinary eutectics formed by τ_1 with the TiCu, ZrCu and γ phases cannot be accepted because of inconsistencies with geometric thermodynamic rules.

According to calculation, the liquidus temperature of the β phase decreases with increasing Cu content up to the point E_5, which corresponds to the minimum liquidus temperature of the ternary system. The main feature of liquidus surface in the central portion of the ternary system is the existence of a primary crystallization surface for the τ_1 ternary phase with a melting temperature lower than the melting temperatures of the coexisting binary phases. Such a feature creates an overall liquidus depression in the central portion of the ternary system, (Figs. 8 to 11) which explains the wide range of glass formation. Between 925 and 875°C, the liquid phase field branches into two topologically non-connected regions, as shown in Fig. 9. One of them corresponds to the liquidus depression observed in the Zr_2Cu-Ti_2Cu composition line according to the results of [1990Che]. The elongated region of liquid parallel to the Cu-Ti edge coincides with location of the lowest liquidus in any of the copper containing binaries bounding the ternary system.

The solidus projection, Fig. 7, is constructed based on the thermodynamic calculation of [2003Arr]. Five tie lines of maximum solidus temperatures exist in the system: TiCu + $Zr_{14}Cu_{51}$, τ_1 + ZrCu, τ_1 + $Zr_{14}Cu_{51}$, τ_1 + $\gamma^{a)}$ and τ_1 + $\gamma^{b)}$, where $\gamma^{a)}$ and $\gamma^{b)}$ are γ phase enriched with Zr or with Ti, respectively, which correspond to three-phase invariant equilibria of eutectic type. Four of the tie-lines show equilibria involving the ternary compound τ_1, and their temperatures, in some cases (τ_1 + $Zr_{14}Cu_{51}$ and τ_1 + γ^{b}) are

noticeably higher than those of the adjoining three phase planes. The three-phase τ_1 + $\gamma^{a)}$ + β alloys demonstrate the lowest solidus temperature in the ternary system.
Isothermal planes $TiCu_4 + Ti_2Cu_3 + TiCu_2$ at 869°C and $Ti_2Cu_3 + TiCu_2 + Ti_3Cu_4$ at 874°C are not exposed because of their degeneration to lines due to the assumption of zero content of Zr in the Cu-Ti binary phases.

Isothermal Sections

Calculated isothermal sections for temperatures from 703 to 925°C are given in Figs. 8 to 14. Isothermal sections for 703, 875 and 925°C, Figs. 14, 9 and 8, respectively, are taken from [2003Arr]. The others are calculated in the present assessment on the basis of the thermodynamic assessment of [2003Arr]. Calculated and experimental sections at 750°C are compared in Figs. 13a and 13b.
The partial isothermal section at 750°C was investigated by [1960Bun, 1961Enc]. Twenty one ternary alloys containing up to 30 mass% Zr and up to 40 mass% Cu were prepared in a non-consumable arc furnace under argon. The alloys were homogenized for 48 h at 825°C prior to annealing at 750°C for 5 d and then additionally for 7 d in order to check that the alloys had reached equilibrium. Specimens were studied by metallographic examination and X-ray diffraction. The existence of the three-phase $\alpha + \beta + Ti_2Cu$ field was established in the Ti rich corner of the section, Fig. 13b. Satisfactory agreement between the calculated and experimental data can be seen.
The isothermal section at 703°C and 50 to 100 at.% Cu was studied by [1988Woy]. The alloys were annealed at 703°C for 14 d and quenched into iced brine. The samples were analyzed using optical microscopy and EMPA. The phase relations were determined by the fitting of the corresponding three-phase triangles because the two-phase regions were very narrow. The authors report that the extent of phase penetration into the ternary system from the respective binary phases is rather limited and generally, does not exceed 5 at.%. However, TiCu and Zr_7Cu_{10} are exceptions, in that they remain stable in the ternary system up to nearly 10 at.% of the third component. It is worth noting that, besides these two binary phases, homogeneity ranges can be suggested only indirectly for the Zr_3Cu_8, ZrCu, and Ti_3Cu_4 binary phases. The other binary intermediate phases have no extension into the ternary system. One of the dominant features of the 703°C section is the presence of the ternary τ_1 phase, which coexists in equilibria with most of the stable phases at this temperature. The $\tau_1 + \alpha + \gamma$ and $\tau_1 + \beta + \gamma$ three-phase fields reported by [1988Woy] contradict the experimental results of [1961Enc] and the calculation of [2003Arr]. The results of [1988Woy] suggest that equilibrium was not achieved in their samples (taking into account that $\tau_1 + \beta + \gamma$ phase field exists at higher temperatures, as one can see, for example, for 827 and 810°C in Figs. 11, 12, respectively). There is no agreement between the experimental data of [1988Woy] and the calculations of [2003Arr] in the Cu rich corner of the phase diagram, in which the existence of $Zr_7Cu_{10} + Ti_2Cu_3$ and $Zr_7Cu_{10} + Ti_3Cu_4$ fields were reported by [1988Woy] at 703°C instead of the alternative $TiCu + Zr_{14}Cu_{51}$, $Zr_{14}Cu_{51} + \tau_1$ or $Zr_3Cu_8 + \tau_1$ obtained by the calculation. The isothermal ternary section for 703°C as calculated by [2003Arr] is shown in Fig. 14. The calculated isothermal sections at 750 and 703°C differ in the compositions of the α, β and γ phases in the respective three-phase equilibria, and by the existence of $Zr_{14}Cu_{51} + TiCu_4$ equilibria instead of $ZrCu_5 + Ti_3Cu_2$.

Temperature – Composition Sections

Two vertical sections, Zr_2Cu-Ti_2Cu and ZrCu-TiCu, are given in Figs. 15 and 16 as results of calculations performed in the current assessment. The Zr_2Cu-Ti_2Cu vertical section given in Fig. 15 differs from the corresponding one by [2003Arr] near the Zr_2Cu and Ti_2Cu ordinates. The phase equilibria in the Zr rich portion of the section presented by [2003Arr] which shows a transgression of the phase rule is corrected. The Ti rich part the diagram was corrected taking into account the congruent melting of Ti_2Cu, and the topology of the Zr rich part was similar to that in the present calculations. This part is shown by a dashed line. The Zr_2Cu-Ti_2Cu and ZrCu-TiCu sections were studied experimentally by [1990Che] and [1992Kov], respectively. [1990Che] studied thirteen alloys along Zr_2Cu-Ti_2Cu section, both in the as-cast and annealed (at 700°C) conditions. It was established that the mutual substitution of Ti and Zr in Ti_2Cu and Zr_2Cu leads to a decrease in the liquidus temperature down to 830°C at 36.7 at.% Zr. The precipitation of a third phase was observed in as-cast alloys at Zr contents of 27 to 36 at.% Zr, which was identified as a $MgZn_2$ type

Laves phase. A continuous γ solid solution was found below 830°C. Generally, good agreement was achieved between the experimental liquidus and solidus points determined by [1990Che] and the calculated solidus and liquidus lines. The composition-temperature range in which the τ_1 ternary phase was observed by [1990Che] corresponds to that where the τ_1 phase coexists with other phases of the ternary system below the solidus over some temperature intervals according to the calculation of [2003Arr]. The minimum solidus temperature after [2003Arr] is about 805°C. The Zr_2Cu-Ti_2Cu temperature composition section calculated by [2003Arr], Fig. 15, is in acceptable agreement with the experimental data of [1990Che]. The cut of the solidus isotherms of the U_8 and E_5 invariant reactions are seen at the middle of the section. The presence of the β phase together with γ solid solution in the calculated section is connected with the fact that the composition of the Zr_2Cu and Ti_2Cu compounds are not strictly stoichiometric. It is important to note that the calculated β phase fraction in the β + γ phase field is very small, from 10^{-3} to 10^{-9}. The experimental detection of this phase would have been too difficult owing to the small amount.
[1992Kov] investigated twenty one as-cast and annealed (at 700°C) alloys of the ZrCu-TiCu section and the corresponding temperature-composition section was reported. Satisfactory agreement is observed between the experimental liquidus points detected by [1992Kov] and calculated liquidus lines in the vertical section. According to [1992Kov], the τ_1 phase (defined as a λ_1 phase) forms congruently at 867°C and 25 at.% Ti and has a homogeneity range along the ZrCu-TiCu section, which extends between 30 at.% Ti (at 842°C) and 12.5 at.% Ti (at ~820°C). [1992Kov] reports a limiting solubility of 4 at.% Zr in TiCu at solidus. Unfortunately, the interpretation of the phase relations of the section by [1992Kov] is in contradiction with the experimental data of [1988Woy] as well as with the calculation of [2003Arr]. Figure 16 shows the ZrCu-TiCu temperature-composition section across the whole concentration range calculated according to the thermodynamic assessment of [2003Arr]. Enlarged parts of the calculated ZrCu-TiCu section are shown in Figs. 17 and 18.

Thermodynamics

Experimental information on the thermodynamic properties of the ternary phases is not available. A thermodynamic assessment of the Cu-Ti-Zr system was carried out by [2003Arr] using the Calphad approach. Binary interaction parameters for the Cu-Ti, Cu-Zr and Ti-Zr systems were taken from previous work [1996Kum, 1994Zen, 1994Kum]. The ternary parameters for the liquid and β phases and the thermodynamic description for the γ- and ternary τ_1 phases were determined from the experimental data on phase relations after [1988Woy, 1990Che]. The ternary parameters for the solution phases (liquid and β) take into account their mixing enthalpy only. The Gibbs free energy of the γ phase was described in the framework of the two sublattice model. The ternary τ_1 phase and all of the binary phases (except γ, TiCu and $TiCu_4$) were represented by [2003Arr] as stoichiometric compounds. For the TiCu and $TiCu_4$ phases, the homogeneity ranges in the binary systems only were taken into account in the calculation. Good agreement was obtained between the calculated temperatures for the invariant reactions in the central part of the system with the data reported by [1988Woy] based on the Transient Liquid Phase bonding technique. However, some discrepancies between the calculated and experimental ternary isothermal sections at 703°C after [1988Woy] are observed: continuous γ solid solution according to calculation (in agreement with [1990Che]) instead of $\tau_1 + \alpha + \gamma$ or $\tau_1 + \beta + \gamma$ phase fields after [1988Woy]; phase equilibria $\tau_1 + Zr_3Cu_8$ instead of $Ti_3Cu_4 + Zr_7Cu_{10}$ or $Ti_2Cu_3 + Zr_7Cu_{10}$ after [1988Woy] and others. It is worth noting that the three-phase equilibria in the composition region 0 to 50 at.% Cu assumed by [1988Woy] do not correspond to the equilibrium conditions at 703°C if taking into account the results of [1990Che]. More experimental information on the area enriched by Cu is needed. It also appears to be necessary to assess the reliability of the experimental data at 703°C for the ternary system at high Cu contents. Experimental investigations of the thermodynamic properties of the ternary τ_1 phase, γ phase and liquid alloys are required.

Notes on Materials Properties and Applications

The Cu-Ti-Zr system is well known as a basic system for the preparation of ternary and multicomponent amorphous alloys by rapid quenching from the liquid. Figure 19 shows the experimentally determined glass forming range in Cu-Ti-Zr alloys compiled from different literature sources. It can be seen that glass

forming range occurs in the central portion of composition triangle. Preparation of amorphous alloys by different techniques is considered in [1988Mas, 1990Che, 1992Kov, 1999Lee, 2001Ino, 2002Kas, 2002Lou, 2004Par]. In [1988Mas, 1990Che, 1992Kov, 2001Ino, 2002Kas, 2002Lou, 2004Par], thin ribbon alloy samples were prepared by a melt spinning technique. A pulsed laser quenching technique was used by [1988Mas]. The amorphous $Cu_{90-x}Zr_xTi_{10}$ (x = 20-80), $Cu_{80-x}Zr_xTi_{20}$ (x = 30-50), $Cu_{90-x}Zr_xTi_{10}$ (x = 30-40) and $Cu_{40}Zr_{20}Ti_{40}$ alloys were successfully synthesized by mechanical alloying of mixtures of crystalline Cu, Ti, and Zr powders using a high energy ball milling technique [1999Lee]. These ranges are similar to those for amorphous alloys produced by melt spinning or argon atomization techniques. Ternary bulk amorphous alloys were prepared from the melt by an injection casting technique [1992Kov, 2004Par]. [2001Ino] reported that Cu based bulk glassy alloys of the composition $Zr_{30}Ti_{10}Cu_{60}$ with a rod diameter of 4 mm can be formed by copper mold casting. The alloys had a fracture strength of 2050 to 2160 MPa and plastic elongation of 0.8 to 1.7%. However, only X-ray diffraction was used to characterize the samples. [2002Lou] further studied the microstructure of samples annealed at various stages using TEM. The formation of nanocrystals in the annealed samples was observed. An electron microscopy study by [2002Kas] on both as-cast and as-spun $Zr_{30}Ti_{10}Cu_{60}$ samples clearly demonstrated that as-prepared samples contain a significant volume fraction (about 5-10%) of nanocrystals with diameters ranging from 5 to 15 nm. Thus, the as-prepared ternary samples can by classified as a nanocomposite: nanocrystals embedded in an amorphous matrix. In [2003Jia], microscopic structures and heat release under heating of as-prepared and annealed $Zr_{30-x}Ti_{10+x}Cu_{60}$ alloys (x = 0-10) were studied by TEM, X-ray diffraction and DSC measurements. The first crystalline phase formed during constant rate heating (0.33 $K \cdot s^{-1}$ under flow of purified argon) is a $Zr_{14}Cu_{51}$-like phase with nanometer-sized grains. The first exothermic peak found on DSC curves corresponds to the amorphous-to-nanocrystalline $Zr_{14}Cu_{51}$-like phase transition. The second crystalline phase is also hexagonal, space group $P6_3/mmc$, and is related to the second exothermic peak found in the DSC curves.

Amorphous alloys of the Cu-Ti-Zr system are widely used as filler materials for the brazing of titanium and titanium alloys [1994Bot, 1998Hir, 2001Kun] as well as for the brazing of ceramic-metal composite materials [1992Nak].

Couples of Pd-Ti/Pd-Ti (ASTM grade 7) and 6Al-Ti-4V/6Al-Ti-4V alloys (mass%) were brazed in a vacuum furnace using rapidly solidified amorphous $Zr_{25}Ti_{25}Cu_{50}$ brazing foil [1994Bot]. The tensile strength, fatigue resistance and microstructure of the joints were studied by X-ray diffraction analysis, energy-dispersive spectroscopy and scanning microscopy. The tensile strength of the joint material is close to that of base metal. The fatigue properties of Pd-Ti joints do not differ from those of this base metal. The microstructure and mechanical properties of the brazed joints depend on the brazing cycle conditions: a fine lamellar eutectic joint microstructure consisting of (αTi) and the γ phase is observed after brazing a 6Al-Ti-4V alloy at 900°C for 10 min followed by rapid cooling. This brazing operation results in high strength joints. Brazing at temperatures higher than 900°C and/or with a relatively low cooling rate results in a coarse dendritic microstructure consisting of the γ phase and hexagonal τ_1 phase. Fine precipitates of the τ_1 phase in the α phase matrix were also observed in the transition area between the base metal and the joint. Joints with such microstructures are brittle and have a low strength. It was shown that rapid cooling suppresses formation of the brittle τ_1 phase, thus resulting in high mechanical properties of the brazed joint.

Commercial purity Ti and $Zr_{90}Ti_{10}$ alloy were brazed with amorphous 25Ti-25Zr-50Cu filler metal using Ar gas shielding [1998Hir]. To obtain a joint strength of 400 MPa, the Ti brazes required a brazing temperature of 920°C and a holding time of 120 s. Under these conditions, fracture occurred in the base metal. The $Zr_{90}Ti_{10}$ joint brazed at 880°C and 900°C had a joint strength of approximately 400 MPa for a holding time of 300 ks and were fractured in the base metal after 600 s. This difference in the brazing properties was explained by the microstructural evolution of the brazing filler metals during brazing on the basis of the liquidus projection of the Cu-Ti-Zr ternary system. The investigations were carried out using SEM, X-ray diffractometry and TEM.

The reaction mechanism between Ti and Ni under brazing using an amorphous Cu-Ti-Zr alloy filler metal was investigated by [2000Oht]. The dissolution of the base metal in the liquid filler metal was completed rapidly: in about 60 s at 852°C and 877°C, and for 120 s at 927°C. The dissolution of the titanium base metal is three times that of nickel base metal. The maximum width of the bonded interlayer was related to the

bonding temperature. The Cu-Ti and Ni-Ti intermetallic compound layers formed at the interface of the titanium base metal and the bonded interlayer.
A Ni-Ti shape memory alloy was brazed to commercial pure Ti with Cu-Ti-Zr amorphous filler [2001Kun]. The brazing temperature was higher than 920°C. The effect of brazing condition on reaction layer formation as well as on the joint strength was investigated.
Cu-Ti-Zr amorphous foil was used as insert metal to bond rod shaped specimens with diameters between 10 and 50 mm to alumina ceramics and stainless steel by a diffusion bonding method. Bonding of the materials was possible at 860-880°C.
[1990Che] studied the properties of amorphous alloys along the Zr_2Cu-Ti_2Cu section. Thirteen alloys were obtained in a glassy state across the whole composition range along the section. The variation with composition of electroresistance ρ, microhardness H, embrittlement temperature T_b, and critical thickness d_c of the amorphous alloys along the Zr_2Cu-Ti_2Cu section is shown in Fig. 20. Amorphous alloys with 18-44 at.% Zr have the maximum values of d_c = 200-250 μm. The concentration dependence of critical thickness of the amorphous alloys along the ZrCu-TiCu section was investigated by [1992Kov]. The results of the study are shown in Fig. 21. The break in the d_c dependence corresponds to the composition of the bulk amorphous alloy $Zr_{40}Ti_{10}Cu_{50}$.
The influence of wheel speed on the glass forming ability and thermal behavior of $Zr_{20}Ti_{20}Cu_{60}$ amorphous ribbons was studied by [2004Rev]. The DSC measurements revealed that the higher the wheel speed, the higher the glass transition temperature T_g and crystallization temperature. Independent of wheel speed, crystallization takes place in a two-stage process. The microhardness exhibits linear dependence on the crystallized volume fraction. A perfect solute mixtures model of defect-free nanoparticles embedded in an amorphous matrix was used to account for this strengthening mechanism. The crystallization behavior, the thermal stability, and the microhardness of $Zr_xTi_{40-x}Cu_{60}$ amorphous alloys (x = 15, 20, 22, 25, 30) prepared by melt-spinning have been studied by means of differential scanning calorimetry, DTA, X-ray diffraction and microhardness studies [2004Con1]. The addition of Zr does not affect the microhardness of the amorphous alloys, although they exhibited good mechanical properties. The effect of continuous heating and isothermal heat treatment of ductile $Zr_{20}Ti_{20}Cu_{60}$ amorphous ribbons was investigated by [2004Con2]. Upon continuous heating, the alloy exhibited a glass transition, followed by a change to a supercooled liquid region and two exothermic crystallization stages. The decomposition of the amorphous phase was also observed. The first crystallization stage resulted in the formation of a nanocomposite structure with hexagonal $Cu_{51}Zr_{14}$ particles embedded in the amorphous matrix, while in the second crystallization stage, a hexagonal Cu_2TiZr-like phase precipitated. The released enthalpies were 19 $J \cdot g^{-1}$ and 30 $J \cdot g^{-1}$ for both of the crystallization stages.
The experimental studies of materials properties of the Cu-Ti-Zr system are summarized in Table 5.

Miscellaneous

The diagram of metastable crystallization of the amorphous alloys of Zr_2Cu-Ti_2Cu section, Fig. 22, was constructed by [1990Che]. The crystallization of alloys containing less than 20 at.% Zr or Ti runs in one stage from the amorphous to the γ phase. The range of crystallization of the metastable Laves phase τ_1' occupies the central part of the diagram at 20-44 at.% Zr. In this concentration range, the amorphous alloys have highest crystallization temperature T_x = 478°C. At the same time, the maximum temperature of recrystallization of the τ_1' phase to the γ phase is observed at 600°C and 30 at.% Zr.
The kinetics of the amorphous-to-$Zr_{14}Cu_{51}$ phase transformation in an as-cast $Zr_{20}Ti_{20}Cu_{60}$ rod has been investigated by DSC by [2003Cao]. The relative volume fraction of the transformed crystalline phase as a function of annealing time, obtained for 440, 443,450, 455, and 460°C, has been analyzed in detail using a number of nucleation and growth models together with the Johnson-Mehl-Avrami model. A steady-state nucleation rate of the order of 10^{22}-10^{23} nuclei $m^{-3} \cdot s^{-1}$ in the temperature range 440-460°C and activation energy about 550 $kJ \cdot mol^{-1}$ for the phase transformation in the as-cast $Zr_{20}Ti_{20}Cu_{60}$ rod were detected. The crystallization kinetics of ductile $Zr_{20}Ti_{20}Cu_{60}$ ribbons was studied from the isothermal treatment and was analyzed using the Johnson-Mehl-Avrami-Kolmogorov model by [2004Rev, 2004Con2].

References

[1960Bun] Bunshah, R.F., Osterberg, D., Ence, E., Margolin, H., "Further Studies on Active-Eutectoid Alloys of Titanium", *U.S. Dept Comm. Office Tech. Serv., PB Rept*., *161964*, 1-73 (1960) (Crys. Structure, Experimental, Mechan. Prop., Phase Diagram, Phase Relations, 26)

[1961Enc] Ence, E., Margolin, H., "A Study of the Ti-Cu-Zr System and the Structure of Ti_2Cu", *Trans. Metall. Soc. AIME*, **221**, 320-322 (1961) (Crys. Structure, Experimental, Phase Diagram, 9)

[1965Tes] Teslyuk, M.Yu., "Ternary Intermetallic Compounds with Structure of Laves Phases" (in Russian), *Abstract Ph. D. Theses,* L'viv University, L'viv, 16 pp. (1965) (Experimental, Crys. Structure, Theory) cited from abstract

[1969Tes] Teslyuk, M.Yu., "Intermetallic Compounds with Structure of Laves Phases" (in Russian), in "*Intermetallic Compounds with Structure of Laves Phases*", Nauka, Moscow, 1-138 (1969) (Experimental, Crys. Structure, Theory)

[1979Dri] Drits, M.E., Bochvar, N.R., Guzei, L.S., Lysova, E.V., Padezhnova, E.M., Rokhlin, L.L., Turkina, N.I., "Copper-Niobium-Tin" in "*Binary and Multicomponent Copper-Base System*" (in Russian), Nauka, Moscow, 67 (1979) (Review, Phase Diagram, Phase Relations)

[1983Dut] Dutkiewicz, J., Massalski, T.B., "Search for New Amorphous Materials in Ternary Metal Systems", *Konf. Metalozn., (Mater. Konf.)*, **11th**, 308-312 (1983) (Phase Diagram, Experimental) cited from abstract

[1983Mur] Murray, J.L., "The Cu-Ti (Copper-Titanium) System", *Bull. Alloy Phase Diagrams*, **4**(1), 81-95 (1983) (Crys. Structure, Phase Diagram, Phase Relations, Thermodyn., 85)

[1986Kne] Kneller, E., Khan, Y., Corres, U., "The Alloy System Copper-Zirconium. Part I. Phase Diagram and Structural Relations", *Z. Metallkd.*, **77**, 43-48 (1986) (Experimental, Phase Diagram, Crys. Structure, 26)

[1988Mas] Massalski, T.B., Woychik, C.G., Dutkiewicz, J., "Solidification Structures in Rapidly Quenched Copper-Titanium-Zirconium Alloys", *Metall. Trans. A*, **19A**(7), 1853-1860 (1988) (Phase Relations, Phase Diagram, Morphology, Experimental) cited from abstract

[1988Woy] Woychik, C.G., Massalski, T.B., "Phase Diagram Relationships in the System Cu-Ti-Zr", *Z. Metallkd.*, **79**(3), 149-153 (1988) (Experimental, Phase Diagram, Phase Relations, Morphology, 19)

[1990Che] Chebotnikov, V.N., Molokanov, V.V., "Structures and Properties of Amorphous and Crystalline Alloys in the Ti_2Cu-Zr_2Cu Section in the Ti-Zr-Cu System", *Inorg. Mater. (Engl. Trans.)*, **26**(5), 808-811 (1990) (Crys. Structure, Experimental, Phase Diagram, Phase Relations, 7)

[1991Sin] Singh, R., Lawley, A., Freidman, S., Murty, Y, "Microstructure and Properties of Spray Cast Cu-Zr Alloys", *Mater. Sci. Eng.*, **145A**, 243-255 (1991) (Experimental, Crys. Structure, Phys. Prop., 30)

[1992Kov] Kovneristyi, Yu.K., Pashkovskaya, A.G., "Bulk Amorphization of Alloys in the Intermetallic-Containing System Ti-Cu-Zr" (in Russian), in "*Amorphous Glassy Metallic Materials*", Ros. Akad. Nauk, Baikov Inst. Metallurgy, 153-157 (1992) (Experimental, Morphology, Phase Diagram, Phase Relations, 4)

[1992Nak] Nakamura, N., "Development of Ceramic-Metal Composite Materials", *Kenkyu Hokoku - Fukuoka-ken Kogyo Gijutsu Senta*, **1991**(2), 32-36 (1992) (Morphology, Experimental) cited from abstract

[1994Ari] Arias, D., Abriata, J.P., "Cu-Zr (Copper-Zirconium)" in "*Phase Diagrams of Binary Copper Alloys*", Subramanian, P.R., Chakrabarti, D.J., Laughlin, D.E. (Eds.), ASM Materials Park, OH, 497-502 (1994) (Assessment, Phase Diagram, Phase Relations, Thermodyn., 50)

[1994Bot] Botstein, O., Rabinkin, A., "Brazing of Titanium-Based Alloys with Amorphous 25%Ti-25%Zr-50%Cu Filler Metal", *Mater. Sci. Eng. A*, **A188**(1-2), 305-315 (1994) (Morphology, Phase Relations, Experimental) cited from abstract

[1994Kum] Kumar, H., Wollants, P., Delaey, L., "Thermodynamic Assessment of the Ti-Zr System and Calculation of the Nb-Ti-Zr Phase Diagram", *J. Alloys Compd.*, **206**(1), 121-127 (1994) (Phase Relations, Phase Diagram, Thermodyn., Assessment, 32)

[1994Zen] Zeng, K.J., Haemaelaeinen, M., Lukas, H. L., "A New Thermodynamic Description of the Cu-Zr System", *J. Phase Equilib.*, **15**(6), 577-586 (1994) (Phase Relations, Phase Diagram, Assessment, 55)

[1996Kum] Kumar, H., Ansara, I., Wollants, P., Delaey, L., "Thermodynamic Optimisation of the Cu-Ti System", *Z. Metallkd.*, **87**(8), 666-672 (1996) (Assessment, Phase Relations, Thermodyn., 55)

[1998Bra] Braga, M.H., Malheiros, F.M., Castro, F., Soares, D., "Experimental Points and Invariant Reactions in the Cu-Zr System", *Z. Metallkd.*, **89**(8) 541-545 (1998) (Experimental, Phase Diagram, 31)

[1998Hir] Hirose, A., Nojiri, M., Ito, H., Kobayashi, K., "Brazing of Ti Alloys with Ti-Zr-Cu Amorphous Filler Metal", *Int. J. Mater. Prod. Techn.*, **13**(1-2), 13-27 (1998) (Morphology, Phase Relations, Experimental) cited from abstract

[1999Lee] Lee, P.Y., Lin, C.K., Chen, G.S., Louh, R.F., Chen, K.C., "Formation of Cu-Zr-Ti Amorphous Alloys with Significant Supercooled Liquid Region by Mechanically Alloying", *Mat. Sci. Forum*, **312-314**, 67-72 (1999) (Morphology, Experimental) cited from abstract

[2000Oht] Ohta, S., Inoue, K., Nishida, M., Araki, T., "Reaction Mechanism Between Ti and Ni on Brazing Process", *Yosetsu Gakkai Ronbunshu*, **18(**2), 198-207, (2000) (Morphology, Kinetics, Experimental) cited from abstract

[2001Ino] Inoue, A., Zhang, W., Zhang, T, Kurosaka, K., "High-Strength Cu-Based Bulk Glassy Alloys in Cu-Zr-Ti and Cu-Hf-Ti Ternary Systems", *Acta Mater.*, **49**(14), 2645-2652 (2001) (Morphology, Phase Relations, Mechan. Prop., Experimental, 36)

[2001Kun] Kunimasa, T., Seki, M., Yamamoto, H., Nojiri, M., Uenishi, K., Kobayashi, K. F., "Brazing of Ti-Ni Shape Memory Alloy with Pure Titanium", *Zairyo*, **50**(11), 1218-1222 (2001) cited from abstract

[2002Ans] Ansara I., Ivanchenko, V., "Cu-Ti (Cooper-Titanium)", MSIT Binary Evaluation Program, in MSIT Workplace, Effenberg, G. (Ed.), MSI, Materials Science International Services GmbH, Stuttgart; Document ID: 20.11457.1.20, (2002) (Crys. Structure, Phase Diagram, Assessment, 26)

[2002Kas] Kasai, M., Saida, J., Matsushita, M., Osuna, T., Matsubara, E., Inoue, A., "Structure and Crystallization of Rapidly Quenched Cu-(Zr or Hf)-Ti Alloys Containing Nanocrystalline Particles", *J. Phys.: Condens. Matter*, **14**, 13867-13877 (2002) (Crys. Structure, Experimental, Morphology, 13)

[2002Lou] Louzguine, D.V., Inoue, A., "Nanocrystallization of Cu-(Zr or Hf)-Ti Metallic Glasses", *J. Mater. Res.*, **17**(8), 2112-2120 (2002) (Crys. Structure, Phase Relations, Morphology, Experimental, 32)

[2003Arr] Arroyave, R., Eagar, T.W., Kaufman, L., "Thermodynamic Assesment of the Cu-Ti-Zr System", *J. Alloys Compd.*, **351**, 158-170 (2003) (Assessment, Calculation, Phase Relations, Thermodyn., *, #, 21)

[2003Cao] Cao, Q.P., Zhou, Y.H., Horsewell, A., Jiang, J.Z., "Amorphous-to-$Cu_{51}Zr_{14}$ Phase Transformation in $Cu_{60}Ti_{20}Zr_{20}$ Alloy", *J. Phys.: Condens. Matter*, **15**(50), 8703-8712 (2003) (Phase Relations, Kinetics, Experimental, 40)

[2003Jia] Jiang, J.Z., Kato, H., Ohsuna, T., Saida, J., Inoue, A., Saksl, K., Franz, H., Stahl, K., "Origin of Nandetectable X-Ray Diffraction Peaks in Nanocomposite CuTiZr Alloys", *Appl. Phys. Lett.*, **83**(16), 3299-3301 (2003) (Crys. Structure, Experimental, Phase Relations, 27)

[2004Con1] Concustell, A., Revesz, A., Surinach, S., Varga, L.K., Heunen, G., "Microstructural Evolution During Decomposition and Crystallization of the Cu60Zr20Ti20 Amorphous Alloy", *J. Mater. Res.*, **19**(2), 505-512 (2004) (Crys. Structure, Experimental, Kinetics, Morphology, Phase Relations, 34)

[2004Con2] Concustell, A., Zielinska, M., Revesz, A., Varga, L.K., Surinach, S., Baro, M. D., "Thermal Characterization of $Cu_{60}Zr_xTi_{40-x}$ Metallic Glasses (x=15, 20, 22, 25, 30)", *Intermetallics*, **12**(10-11), 1063-1067 (2004) (Morphology, Structure, Kinetics, Mechan. Prop., Experimental, 34)

[2004Par] Park, E.S., Chang, H.J., Kim, D.H., Kim, W.T., Kim, Y.C., Kim, N.J., Kim, Y.W., "Formation of Amorphous Phase in Melt-Spun and Injection-Cast Cu60Zr30Ti10 Alloys", *Scr. Mater.*, **51**(3), 221-224 (2004) (Crys. Structure, Experimental, Morphology, Phase Relations, 16)

[2004Rev] Revesz, A., Concustell, A., Varga, L.K., Surinach, S., Baro, M.D., "Influence of the Wheel Speed on the Thermal Behavior of $Cu_{60}Zr_{20}Ti_{20}$ Alloys", *Mater. Sci. Eng. A*, **A375-A377**, 776-780 (2004) (Morphology, Crys. Structure, Kinetics, Mechan. Prop., Experimental, 34)

[2006Sem] Semenova, E., Sidorko, V., "Cu-Zr (Cooper-Zirconium)", MSIT Binary Evaluation Program, in MSIT Workplace, Effenberg, G. (Ed.), MSI, Materials Science International Services, GmbH, Stuttgart; to be published, (2006) (Crys. Structure, Phase Diagram, Assessment, 31)

Table 1: Investigations of the Cu-Ti-Zr Phase Relations and Structures

Reference	Method/Experimental Technique	Temperature/Composition/Phase Range Studied
[1961Enc]	Optical microscopy, X-ray analysis	< 50 mass% Ti, isothermal section at 750°C
[1983Dut]	Optical microscopy, EMPA	liquidus surface projection, low melting eutectics
[1988Woy]	Optical microscopy, EMPA, Transient Liquid Phase bonding technique	isothermal section at 703°C and >30 at.% Cu, eutectic reactions in central portion of phase diagram
[1990Che]	Optical microscopy, X-ray analysis, differential thermal analysis, measurements of microhardness	Temperature-composition Ti_2Cu–Zr_2Cu section
[1992Kov]	Optical microscopy, X-ray analysis, differential thermal analysis	Temperature-composition TiCu-ZrCu section

Table 2: Crystallographic Data of Solid Phases

Phase/ Temperature Range [°C]	Pearson Symbol/ Space Group/ Prototype	Lattice Parameters [pm]	Comments/References
(Cu), $Zr_xTi_yCu_{1-x-y}$ < 1084.87	*cF*4 *Fm*$\bar{3}$*m* Cu	*a* = 361.46	pure Cu at 25°C [Mas2] *x* = 0.0012 at 968°C and *y* = 0 [1994Zen] *y* = 0.08 at 896°C and *x* = 0 [1996Kum]
β, $Zr_{1-x-y}Ti_xCu_y$ 1854 - 600	*cI*2 *Im*$\bar{3}$*m* W		0 < *x* < 1 in Zr-Ti system [1994Kum, Mas2]
(βZr) 1854 - 863		*a* = 360.90	pure Zr(h) at *T* > 863°C [Mas2] *y* = 0.037 at 997°C and *x* = 0 [1994Zen]
(βTi) 1668 - 882		*a* = 330.65	pure Ti(h) at *T* > 882°C [Mas2] *y* = 0.159 at 1000°C in Cu-Ti system [1996Kum]
α, $Zr_{1-x-y}Ti_xCu_y$	*hP*2 $P6_3/mmc$		0 < *x* < 1 in Zr-Ti system [Mas2, 1994Kum]
(αZr) < 863	Mg	*a* = 323.16 *c* = 514.75	pure Zr(r) at 25°C [Mas2] *y* = 0.002 at 816°C and *x* = 0 [1994Zen]
(αTi) < 882		*a* = 295.06 *c* = 468.35	pure Ti(r) at 25°C [Mas2] *y* = 0.014 at 799°C in Cu-Ti system [1994Kum]
$ZrCu_5$ < 968	*cF*24 *F*$\bar{4}$3*m* $AuBe_5$	*a* = 687.0	[1994Zen, 1991Sin, 1986Kne]
$Zr_{14}Cu_{51}$ < 1113	*hP*68 *P*6/*m* $Gd_{14}Ag_{51}$	*a* = 1124.44 *c* = 828.15	[1994Zen, V-C2]
Zr_3Cu_8 < 891	*oP*44 *Pnma* Hf_3Cu_8	*a* = 786.93 *b* = 815.47 *c* = 998.48	[1994Zen, V-C2]
Zr_7Cu_{10}, $(Zr_{1-x}Ti_x)_7Cu_{10}$ < 935	*oC*68 *C*2*ca* Zr_7Ni_{10}	*a* = 1267.29 *b* = 931.63 *c* = 934.66	0 < *x* < 0.24 at 703°C [1988Woy] [1994Zen, 1994Ari, 1998Bra]
ZrCu 936-704	*cP*2 *Pm*$\bar{3}$*m* CsCl	*a* = 325.87	[1994Zen, 1994Ari, 1998Bra]

Phase/ Temperature Range [°C]	Pearson Symbol/ Space Group/ Prototype	Lattice Parameters [pm]	Comments/References
γ, $(Zr_{1-x}Ti_x)_2Cu$	*tI*6		$0 < x < 1$ [1990Che]
Zr_2Cu	*I*4/*mmm*	$a = 322.04$	[1994Zen, 1994Ari]
< 1011	$MoSi_2$	$c = 1183.2$	
		$a = 324.26$	[1986Kne, 1998Bra]
		$c = 1127.2$	
Ti_2Cu		$a = 295.3$	[1996Kum, V-C2]
< 1012		$c = 1073.4$	[2002Ans]
$TiCu_4$	*oP*20	$a = 452.5$	78.6-80.8 at.% Cu [1996Kum, Mas2,
< 896	*Pnma*	$b = 434.1$	V-C2]
	$ZrAu_2$	$c = 1295$	
$TiCu_2$	*oC*12	$a = 436.3$	[1996Kum, V-C2]
870 - 890	*Cmm*2	$b = 797.7$	
	VAu_2	$c = 447$	
Ti_2Cu_3	*tP*10	$a = 313$	[1996Kum, V-C2]
< 874	*P*4/*nmm*	$c = 1395$	
	Ti_2Cu_3		
Ti_3Cu_4	*tI*14	$a = 313.0$	[2002Ans, V-C2]
< 933	*I*4/*mmm*	$c = 1994$	
	Ti_3Cu_4		
TiCu, $Zr_xTi_{1-x}Cu$	*tP*4	$a = 312.5$	[V-C2]
< 975	*P*4/*nmm*	$c = 591.5$	48.5-51.7 at.% Cu at $x = 0$ [1996Kum]
	TiCu		$0 < x < 0.2$ at 703°C [1988Woy]
			$0 < x < 0.08$ at 842°C [1992Kov]
* τ_1, $ZrTiCu_2$	*hP*12	$a = 513$	$ZrTiCu_4$ (?) [1965Tes, 1969Tes]
	*P*6$_3$/*mmc*	$c = 825$	
	$MgZn_2$		
< 867			25 at.% Zr, 25 at.% Ti, 50 at.% Cu at 867°C; 21 to 37 at.% Zr at 50 at.% Cu at ~ 830°C; 22.5 to 29 at.% Zr at 50 at.% Cu at ~ 630°C [1992Kov] 25 to 30 at.% Zr and 45 to50 at.% Cu at 703°C [1988Woy]
< 883			calculated by [2003Arr]

Table 3: Invariant Four-Phase Equilibria

Reaction	T [°C]	Type	Phase	Composition (at.%)		
				Cu	Zr	Ti
L + TiCu ⇌ Ti_3Cu_4 + $Zr_{14}Cu_{51}$	882	U_1	L	64.5	6.8	28.7
			TiCu	51.3	0	48.7
			Ti_3Cu_4	57.1	0	42.9
			$Zr_{14}Cu_{51}$	78.5	21.5	0
L + Ti_3Cu_4 + $TiCu_2$ ⇌ Ti_2Cu_3	874	D_1(P)	L	73.4	25.2	1.4
			Ti_3Cu_4	57.1	0	42.9
			$TiCu_2$	66.7	0	33.3
			Ti_2Cu_3	60.0	0	40.0
L + $TiCu_2$ ⇌ $TiCu_4$ + Ti_2Cu_3	869	D_2(U)	L	73.7	2.0	24.3
			$TiCu_2$	66.7	0	33.3
			$TiCu_4$	78.7	0	21.3
			Ti_2Cu_3	60.0	0	40.0
L + (Cu) ⇌ $TiCu_4$ + $ZrCu_5$	863	U_2	L	80.1	4.0	15.9
			(Cu)	93.5	0.1	6.4
			$TiCu_4$	81.2	0	18.8
			$ZrCu_5$	83.3	16.7	0
L + $Zr_{14}Cu_{51}$ ⇌ Zr_3Cu_8 + τ_1	861	U_3	L	56.5	33.3	10.2
			$Zr_{14}Cu_{51}$	78.5	21.5	0
			Zr_3Cu_8	72.7	27.3	0
			τ_1	50.0	25.0	25.0
L + γ ⇌ τ_1 + TiCu	856	U_4	L	50.7	14.0	35.3
			γ	33.3	4.1	62.6
			τ_1	50.0	25.0	25.0
			TiCu	49.6	0	50.4
L + $ZrCu_5$ ⇌ $Zr_{14}Cu_{51}$ + $TiCu_4$	855	U_5	L	75.7	4.2	20.1
			$ZrCu_5$	83.3	16.7	0
			$Zr_{14}Cu_{51}$	78.5	21.5	0
			$TiCu_4$	79.6	0	20.4
L ⇌ TiCu + τ_1 + $Zr_{14}Cu_{51}$	855	E_1	L	52.7	14.2	33.1
			TiCu	49.8	0	50.2
			τ_1	50.0	25.0	25.0
			$Zr_{14}Cu_{51}$	78.5	21.5	0
L + Ti_3Cu_4 ⇌ Ti_2Cu_3 + $Zr_{14}Cu_{51}$	854	U_6	L	73.7	4.2	22.1
			Ti_3Cu_4	57.1	0	42.9
			Ti_2Cu_3	60.0	0	40.0
			$Zr_{14}Cu_{51}$	78.5	21.5	0
L ⇌ $TiCu_4$ + Ti_2Cu_3+ $Zr_{14}Cu_{51}$	852	E_2	L	74.2	4.1	21.7
			$TiCu_4$	79.0	0	21.0
			Ti_2Cu_3	60.0	0	40.0
			$Zr_{14}Cu_{51}$	78.5	21.5	0

Reaction	T [°C]	Type	Phase	Composition (at.%)		
				Cu	Zr	Ti
$L + Zr_3Cu_8 \rightleftharpoons \tau_1 + Zr_7Cu_{10}$	845	U_7	L	55.8	36.8	7.4
			Zr_3Cu_8	72.7	27.3	0
			τ_1	50.0	25.0	25.0
			Zr_7Cu_{10}	58.8	41.2	0
$L \rightleftharpoons \tau_1 + ZrCu + Zr_7Cu_{10}$	839	E_3	L	52.3	39.9	7.8
			τ_1	50.0	25.0	25.0
			ZrCu	50.0	50.0	0
			Zr_7Cu_{10}	58.8	41.2	0
$L + \gamma \rightleftharpoons \tau_1 + \beta$	835	U_8	L	34.4	28.8	36.8
			γ	33.3	20.6	46.1
			τ_1	50.0	25.0	25.0
			β	11.6	25.3	63.1
$L \rightleftharpoons \tau_1 + \gamma + ZrCu$	833	E_4	L	44.8	41.9	13.3
			τ_1	50.0	25.0	25.0
			γ	33.3	58.7	8.0
			ZrCu	50.0	50.0	0
$L \rightleftharpoons \tau_1 + \gamma + \beta$	827	E_5	L	35.8	33.7	30.5
			τ_1	50.0	25.0	25.0
			γ	33.3	35.8	30.9
			β	12.2	31.0	56.7
$ZrCu \rightleftharpoons \tau_1 + \gamma + Zr_7Cu_{10}$	720	E_6	ZrCu	50.0	50.0	0
			τ_1	50.0	25.0	25.0
			γ	33.3	63.8	2.9
			Zr_7Cu_{10}	58.8	41.2	0
$TiCu_4 + Zr_{14}Cu_{51} \rightleftharpoons ZrCu_5 + Ti_2Cu_3$	703-750	U_9	-	-	-	-

Table 4: Invariant Two- and Three-Phase Equilibria

Reaction	T [°C]	Type	Phase	Composition (at.%)		
				Cu	Zr	Ti
$L \rightleftharpoons \tau_1$	883	congruent	L	50.0	25.0	25.0
			τ_1	50.0	25.0	25.0
$L \rightleftharpoons TiCu + Zr_{14}Cu_{51}$	885	e_9 (max)	L	61.4	8.2	30.4
			TiCu	50.8	0	49.2
			$Zr_{14}Cu_{51}$	78.5	21.5	0
$L \rightleftharpoons \tau_1 + Zr_{14}Cu_{51}$	879	e_{10} (max)	L	55.0	24.3	20.7
			τ_1	50.0	25.0	25.0
			$Zr_{14}Cu_{51}$	78.5	21.5	0

Reaction	T [°C]	Type	Phase	Composition (at.%)		
				Cu	Zr	Ti
$L \rightleftharpoons \tau_1 + \gamma^{b)}$	869	e_{11} (max)	L	43.6	18.1	38.3
			τ_1	50.0	25.0	25.0
			$\gamma^{b)}$	33.3	7.0	59.7
$L \rightleftharpoons \tau_1$ + ZrCu	841	e_{12} (max)	L	50.0	40.5	9.5
			τ_1	50.0	25.0	25.0
			ZrCu	50.0	50.0	0
$L \rightleftharpoons \tau_1 + \gamma^{a)}$	835	e_{13} (max)	L	42.0	39.9	18.1
			τ_1	50.0	25.0	25.0
			$\gamma^{a)}$	33.3	56.4	10.3

$\gamma^{a)}$ and $\gamma^{b)}$ denote γ phase enriched by Zr or by Ti, respectively

Table 5: Investigations of the Cu-Ti-Zr Materials Properties

Reference	Method/Experimental Technique	Type of Property
[1983Dut]	X-ray analysis, DSC	T_x, T_g of amorphous alloys,
[1988Mas]	X-ray analysis, DSC	T_g of amorphous alloys,
[1990Che]	X-ray analysis, electroresistance tests, microhardness tests	electroresistance ρ, microhardness H, embrittlement temperature T_b, and critical thickness d_c of the amorphous alloys of Zr_2Cu-Ti_2Cu section
[1992Kov]	X-ray analysis, DTA	Critical thickness d_c and critical cooling rates R_c of the amorphous alloys of ZrCu-TiCu section
[1994Bot]	Energy dispersive X-ray spectroscopy, X-ray analysis, SEM, microhardness tests	Microstructure and mechanical properties of brazed joints
[2001Ino]	DSC, mechanical properties tests	Structure of $Zr_{30}Ti_{10}Cu_{60}$ bulk amorphous alloy
[2001Kun]	X-ray analysis, mechanical properties tests	Microstructure and mechanical properties of brazed joints
[2002Kas]	X-ray analysis, anomalous X-ray scattering measurements, high resolution TEM, energy dispersive X-ray spectroscopy	Structure of the as-cast and as-spun $Zr_{30}Ti_{10}Cu_{60}$ amorphous alloy
[2002Lou]	X-ray analysis, TEM, energy dispersive X-ray spectroscopy, DSC	Structure and crystallization of $Zr_{30}Ti_{10}Cu_{60}$ amorphous alloy
[2003Jia]	X-ray analysis, DSC	Structure and crystallization of $Zr_{30-x}Ti_{10+x}Cu_{60}$ amorphous alloys
[2003Cao]	DSC	Kinetic of crystallization of $Zr_{20}Ti_{20}Cu_{60}$ bulk amorphous alloy

Reference	Method/Experimental Technique	Type of Property
[2004Con1]	X-ray analysis, DSC, DTA, microhardness tests	Crystallization, thermal stability and mechanical properties of $Zr_xTi_{40-x}Cu_{60}$ (x = 15, 20, 22, 25, 30) amorphous alloys
[2004Con2]	X-ray analysis, DSC, synchrotron radiation transmission, high resolution TEM	Crystallization and heat release of $Zr_{20}Ti_{20}Cu_{60}$ amorphous alloy
[2004Rev]	DSC	Kinetic of crystallization of $Zr_{20}Ti_{20}Cu_{60}$ amorphous alloy

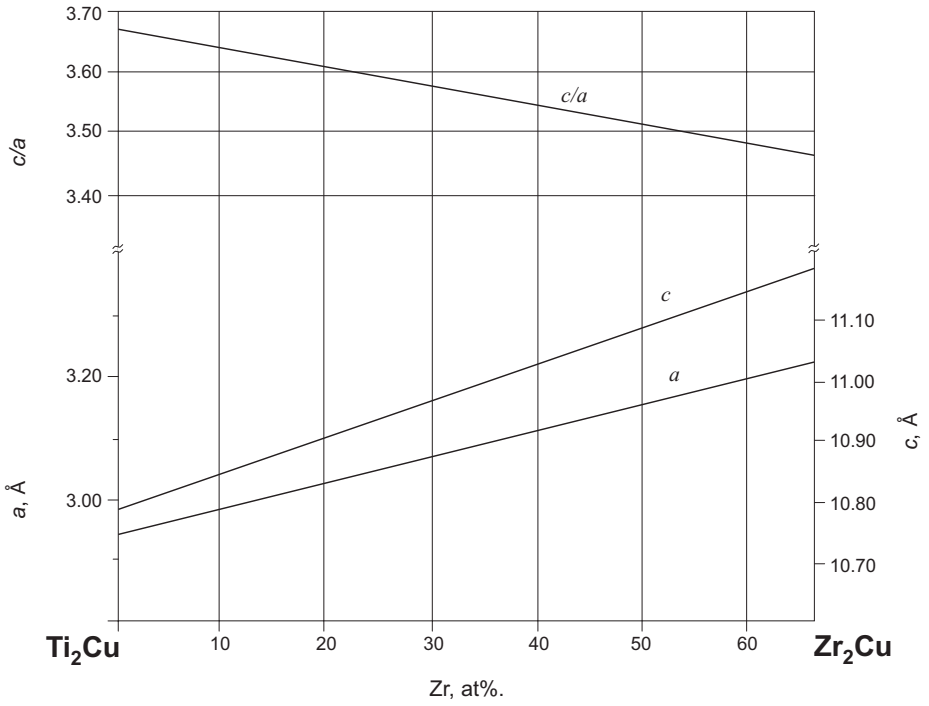

Fig. 1: Cu-Ti-Zr. Lattice parameters of γ phase as function of composition along the Zr_2Cu-Ti_2Cu section

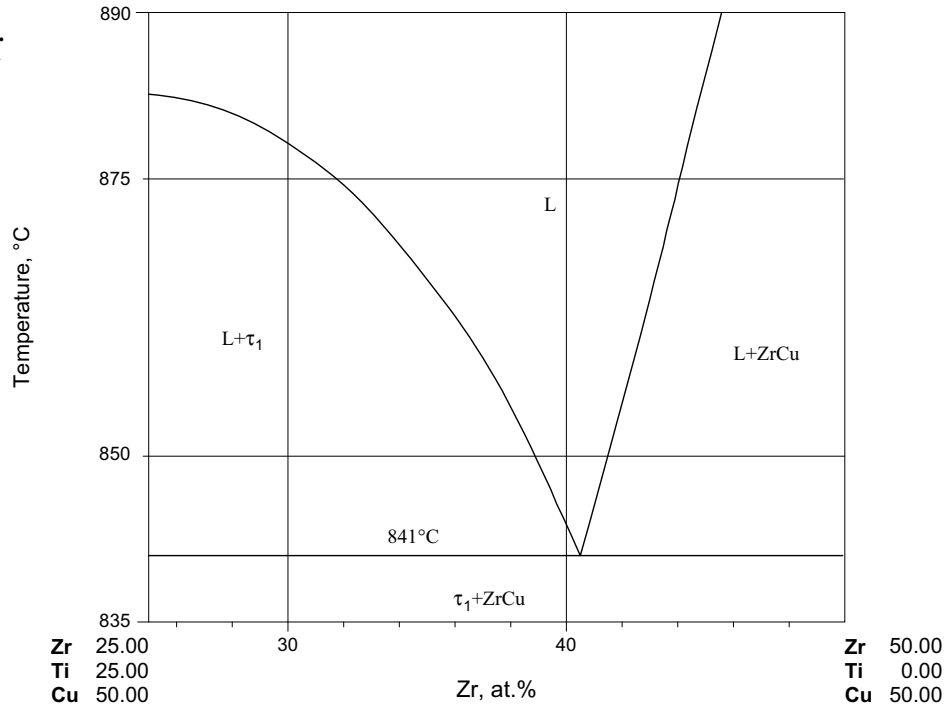

Fig. 2: Cu-Ti-Zr. Calculated partially quasibinary system ZrCu-τ_1

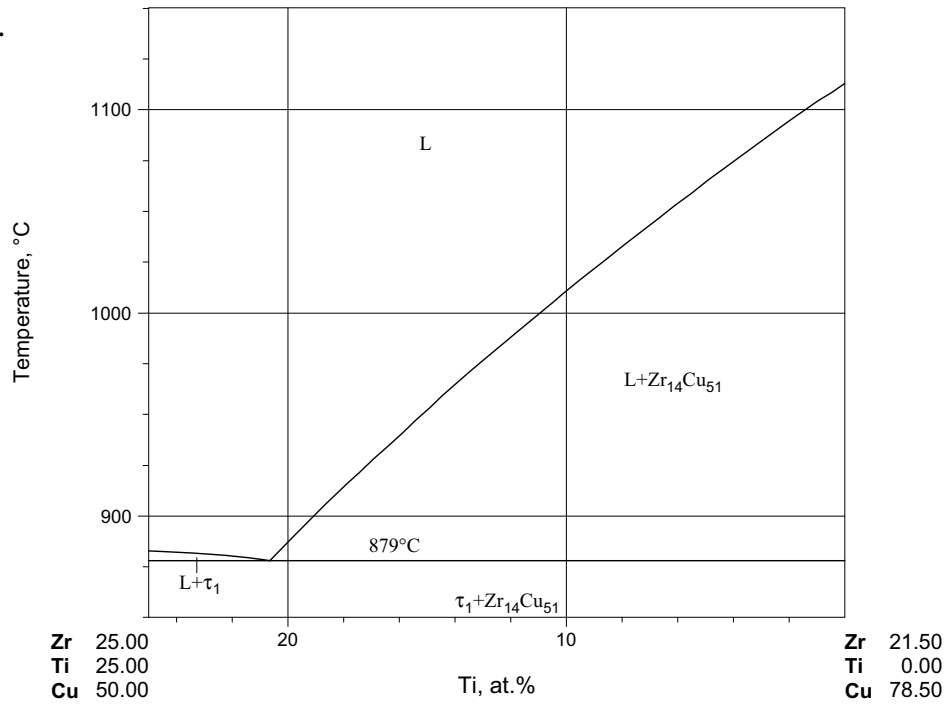

Fig. 3: Cu-Ti-Zr. Calculated quasibinary system τ_1-$Zr_{14}Cu_{51}$

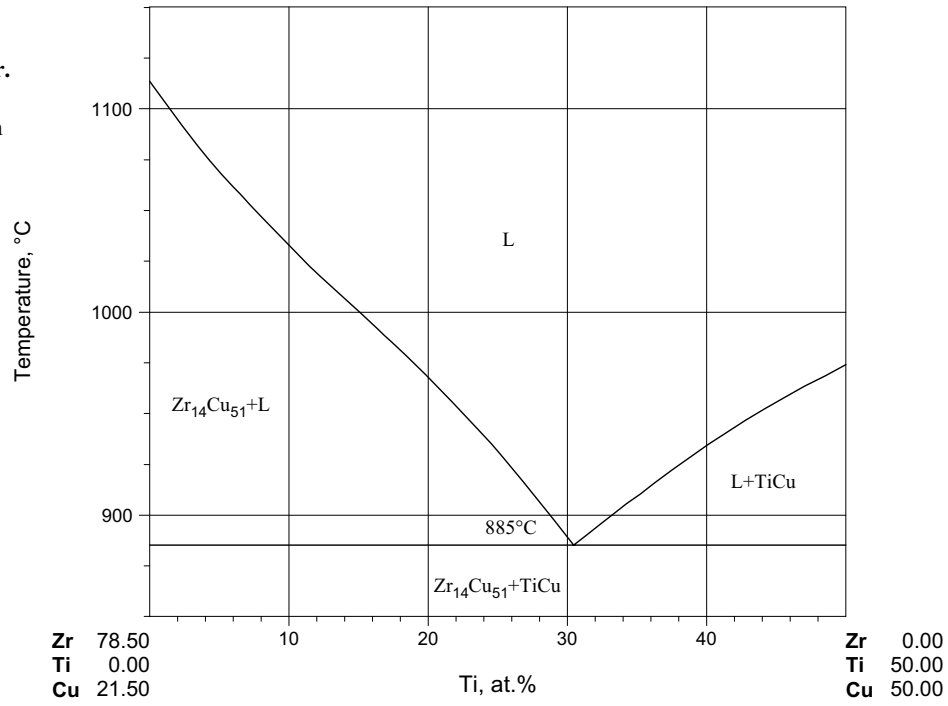

Fig. 4: Cu-Ti-Zr. Calculated quasibinary system $Zr_{14}Cu_{51}$-TiCu

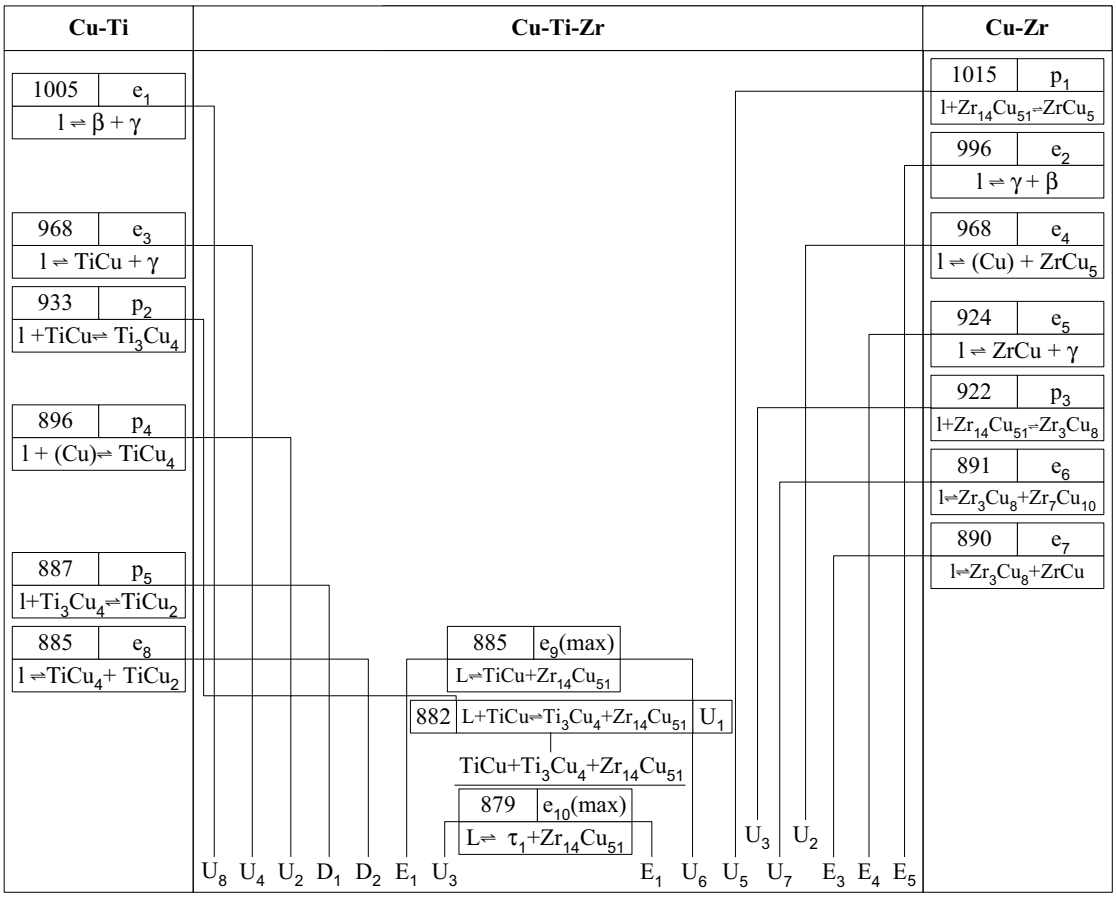

Fig. 5a: Cu-Ti-Zr. Reaction scheme, part 1

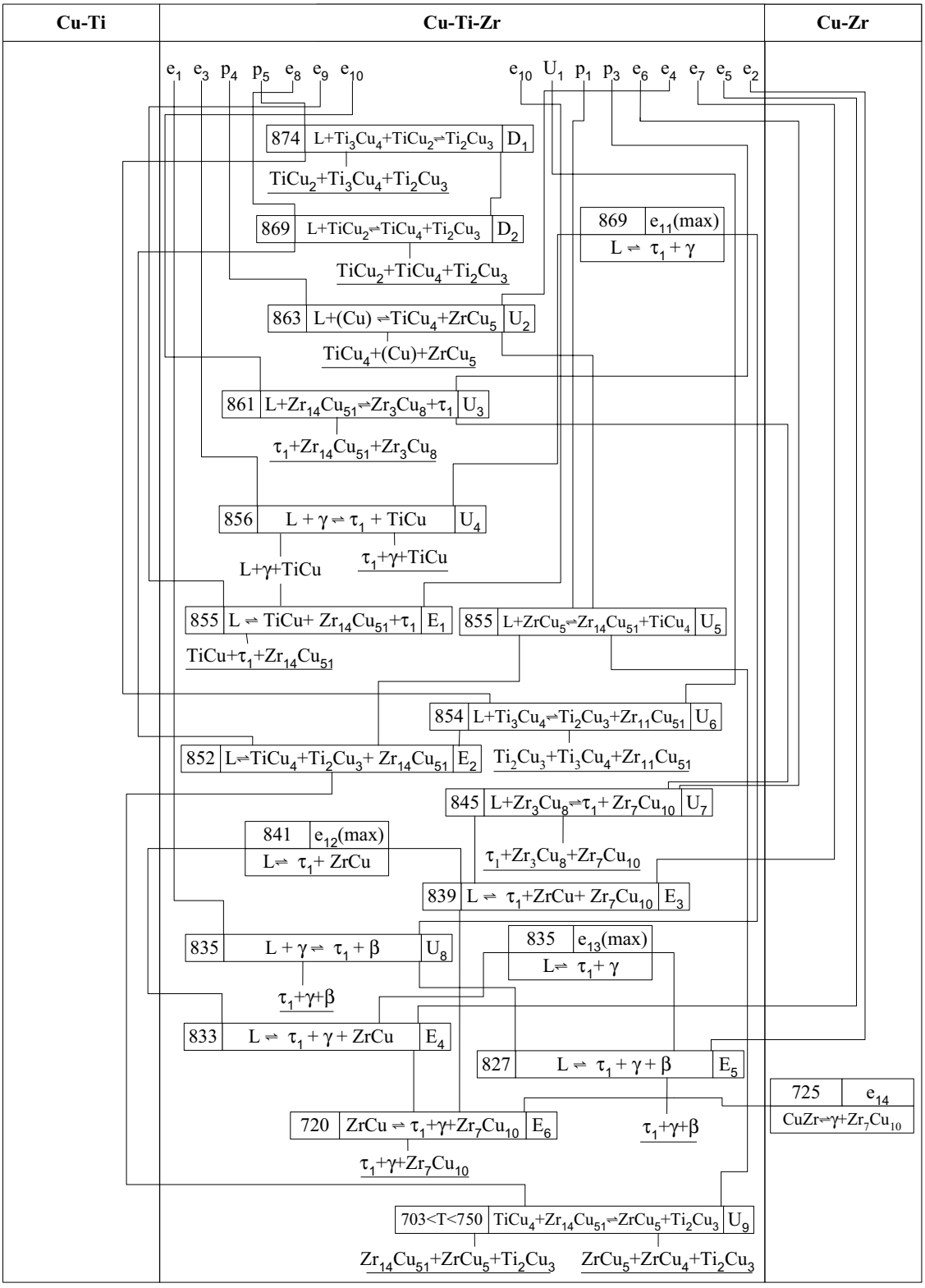

Fig. 5b: Cu-Ti-Zr. Reaction scheme, part 2

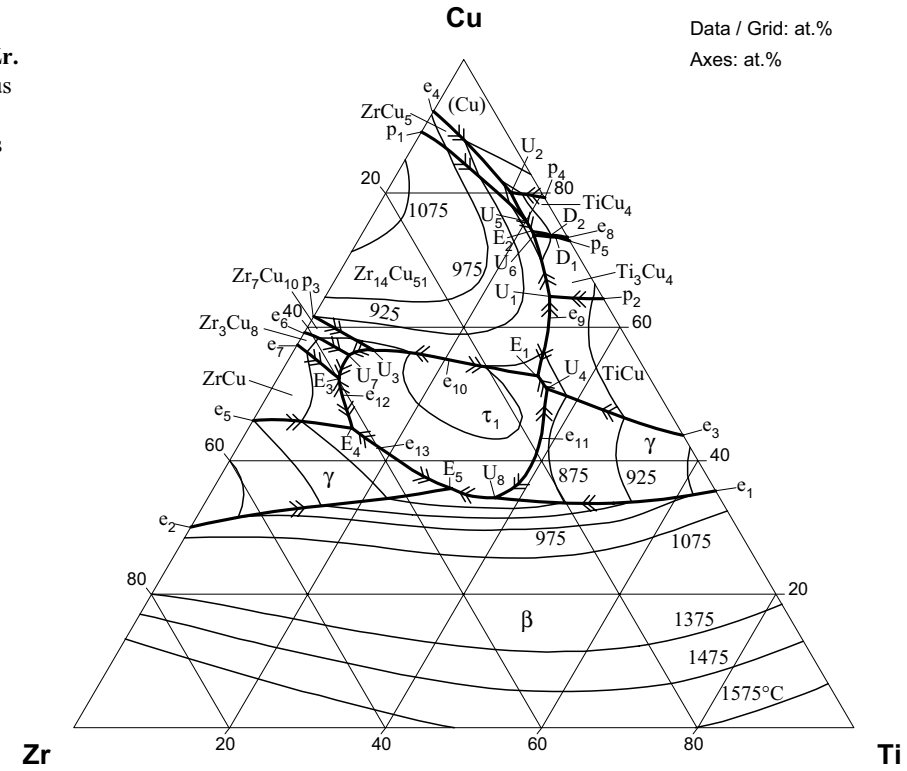

Fig. 6a: Cu-Ti-Zr. Calculated liquidus projection with liquidus isotherms

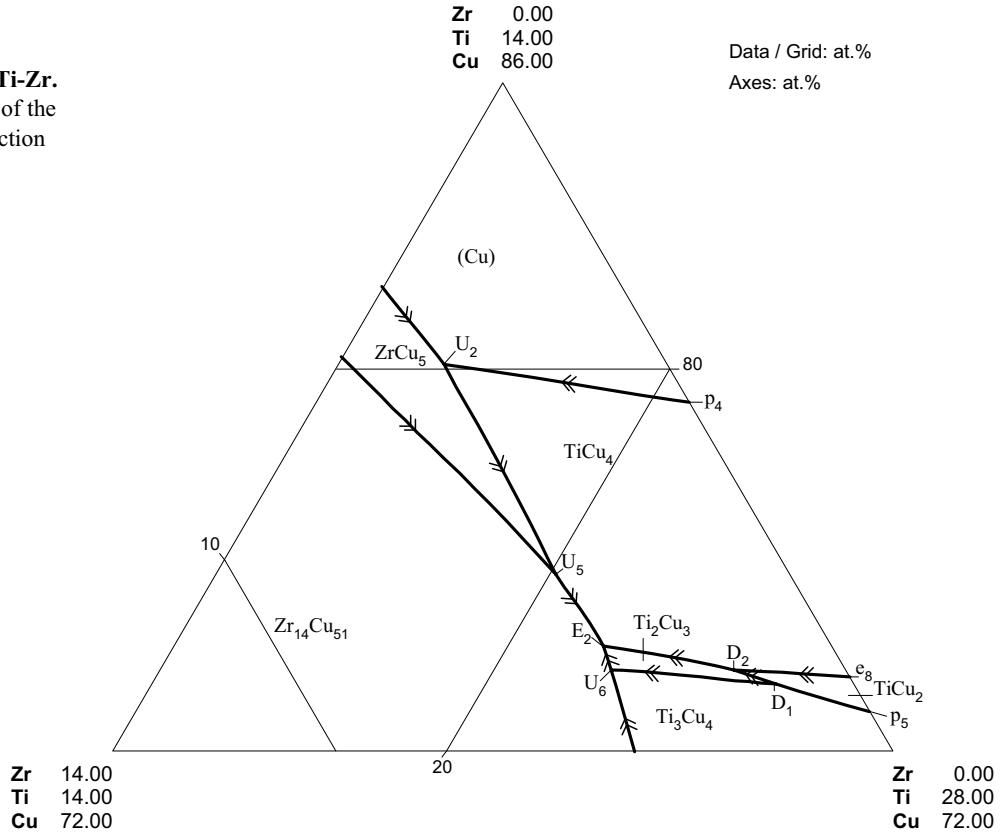

Fig. 6b: Cu-Ti-Zr. Enlarged part of the liquidus projection

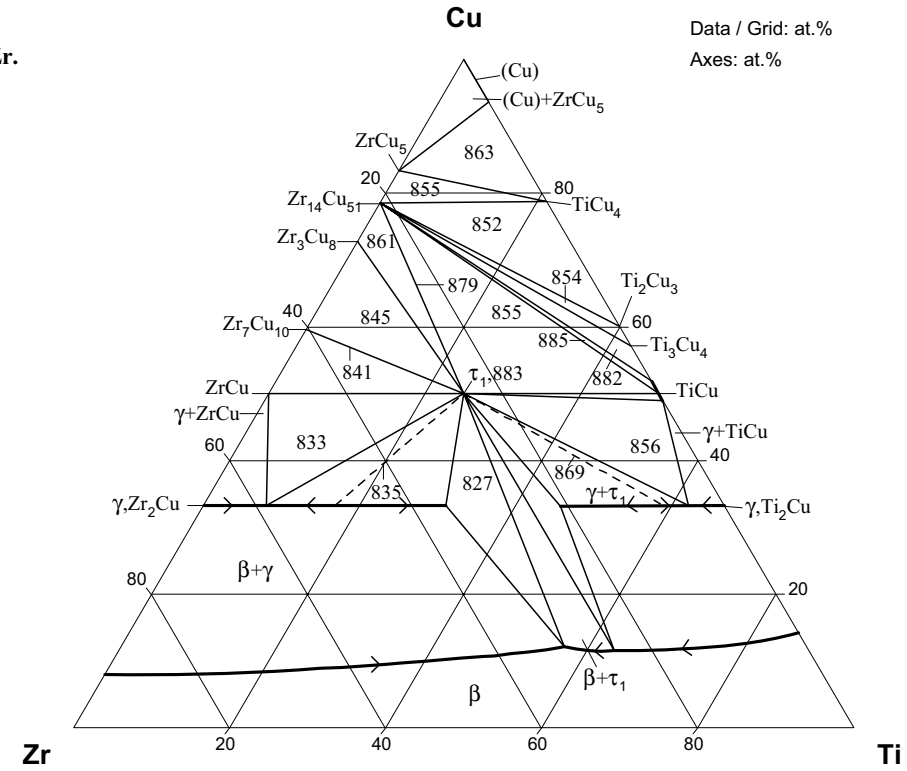

Fig. 7: Cu-Ti-Zr. Solidus surface projection

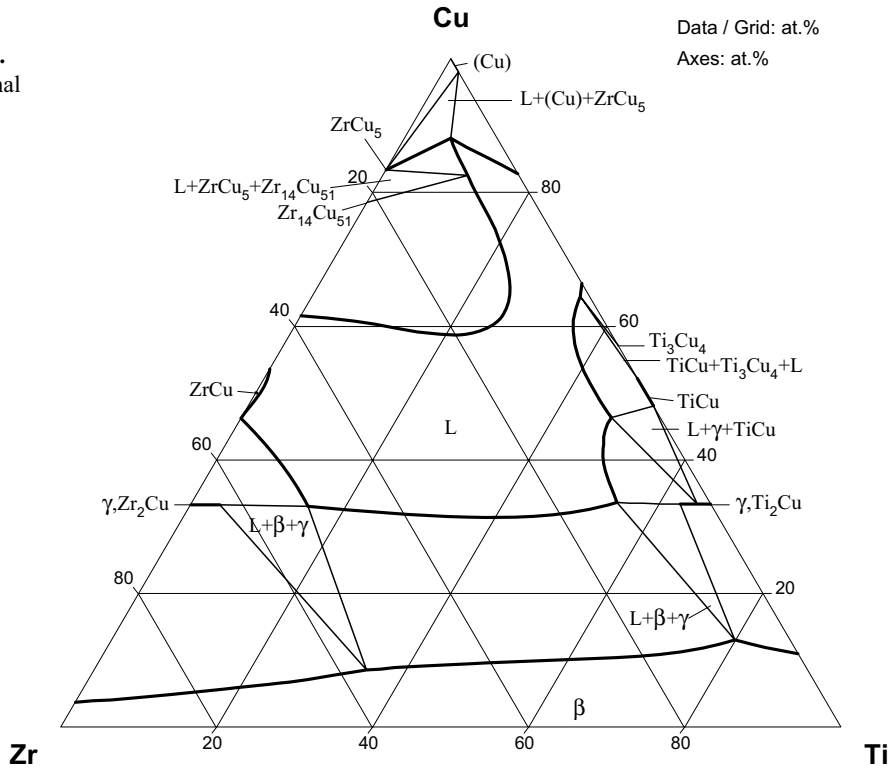

Fig. 8: Cu-Ti-Zr. Calculated isothermal section at 925°C

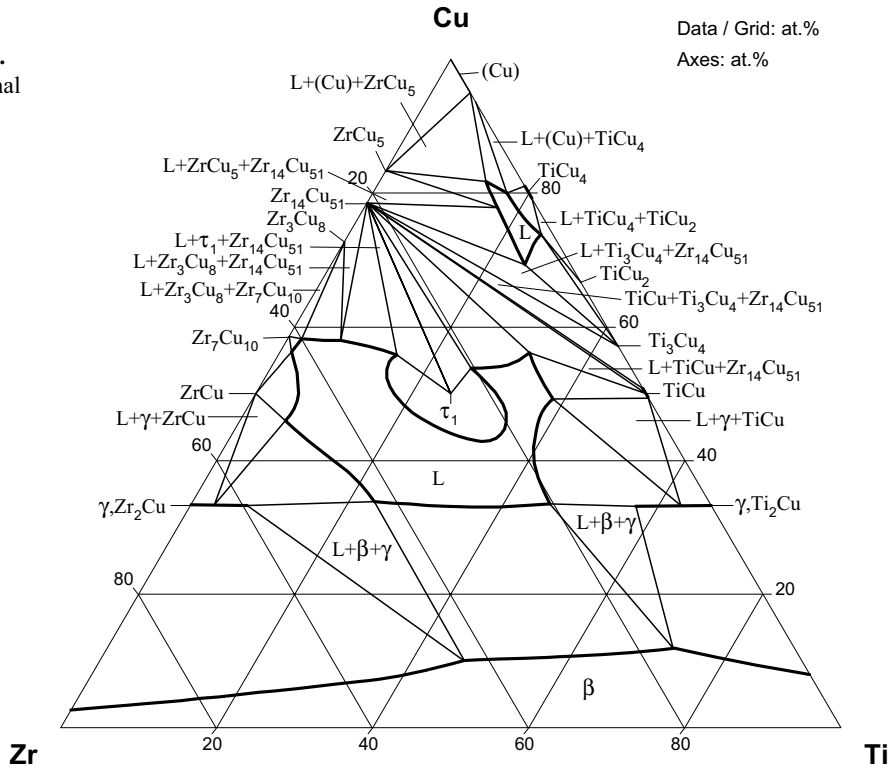

Fig. 9: Cu-Ti-Zr. Calculated isothermal section at 875°C

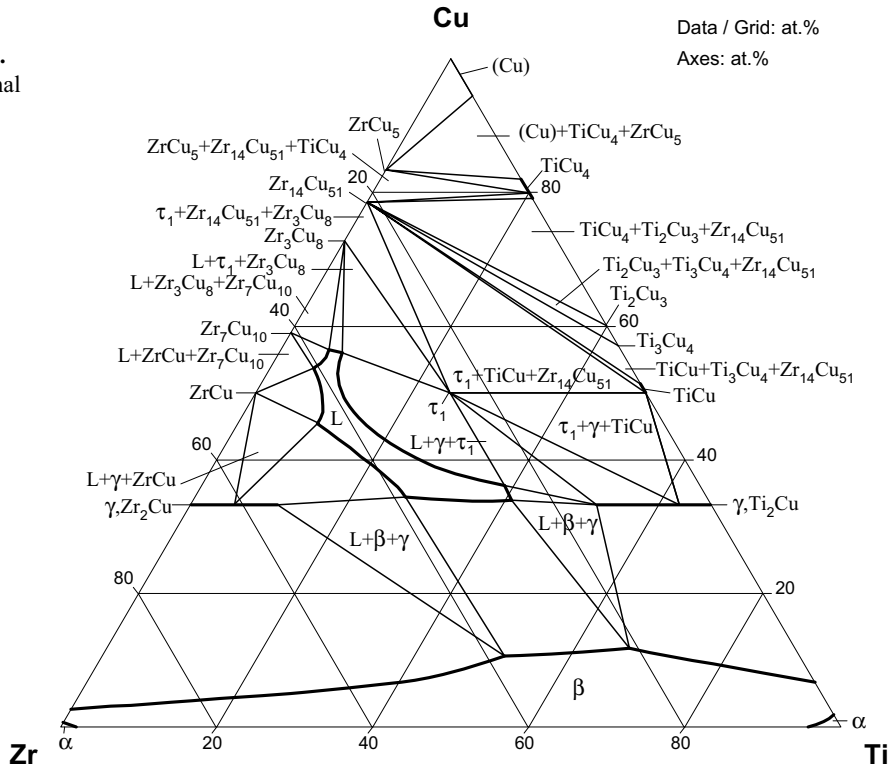

Fig. 10: Cu-Ti-Zr. Calculated isothermal section at 850°C

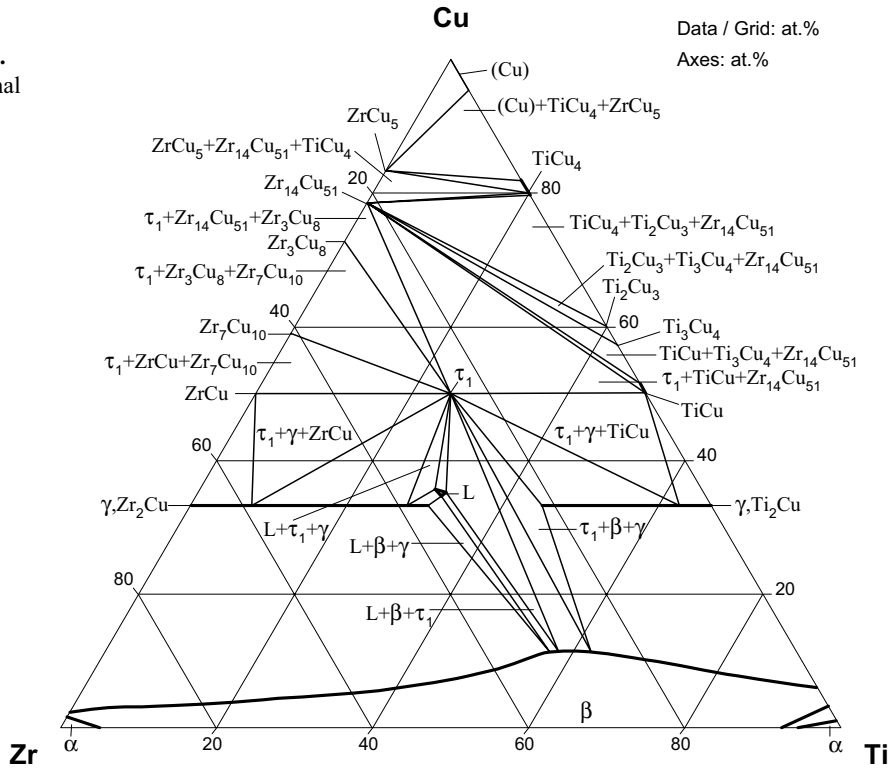

Fig. 11: Cu-Ti-Zr. Calculated isothermal section at 827°C

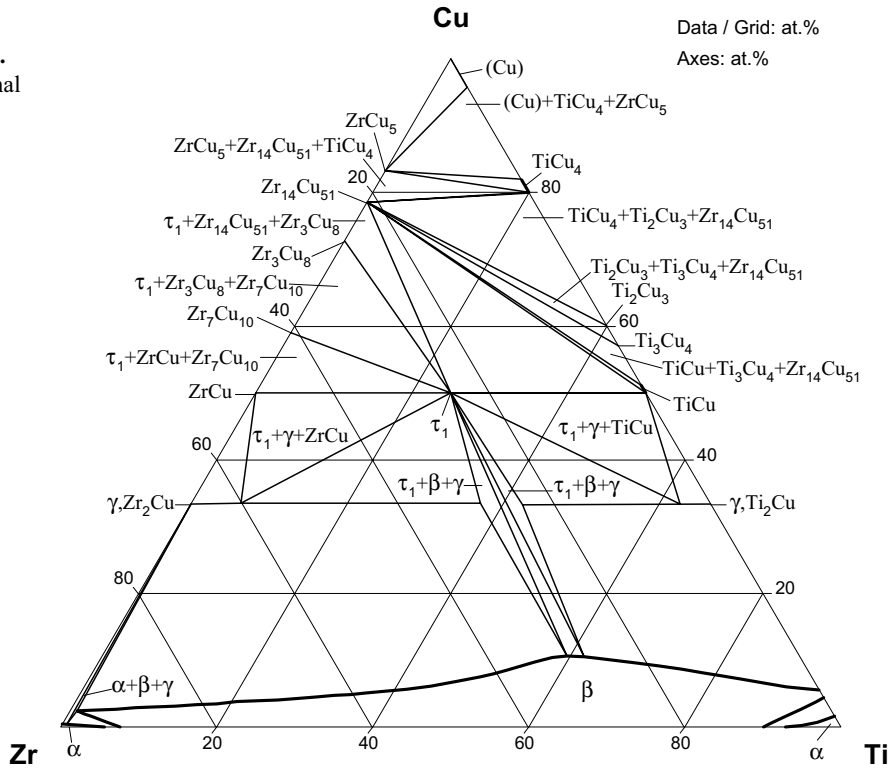

Fig. 12: Cu-Ti-Zr. Calculated isothermal section at 810°C

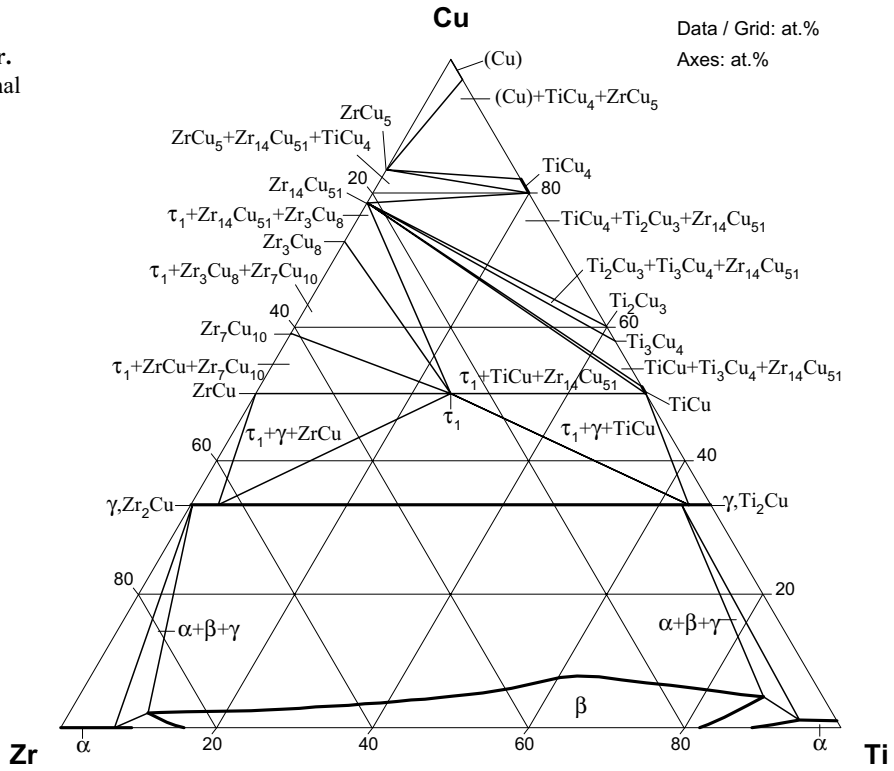

Fig. 13a: Cu-Ti-Zr. Calculated isothermal section at 750°C

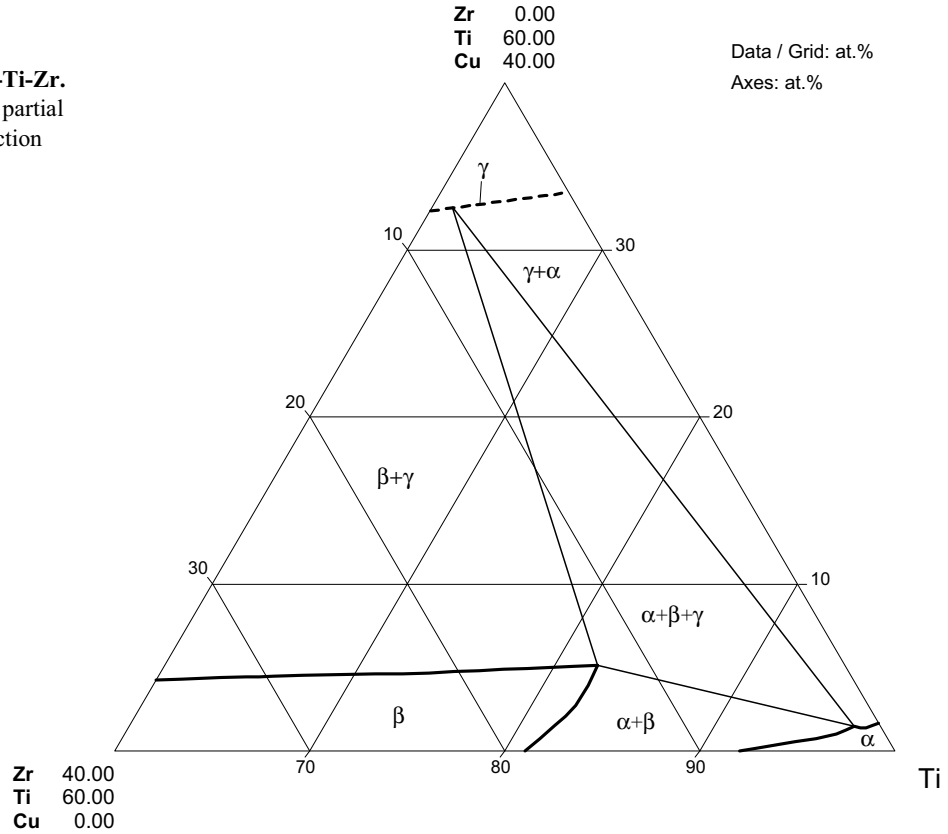

Fig. 13b: Cu-Ti-Zr. Experimental partial isothermal section at 750°C

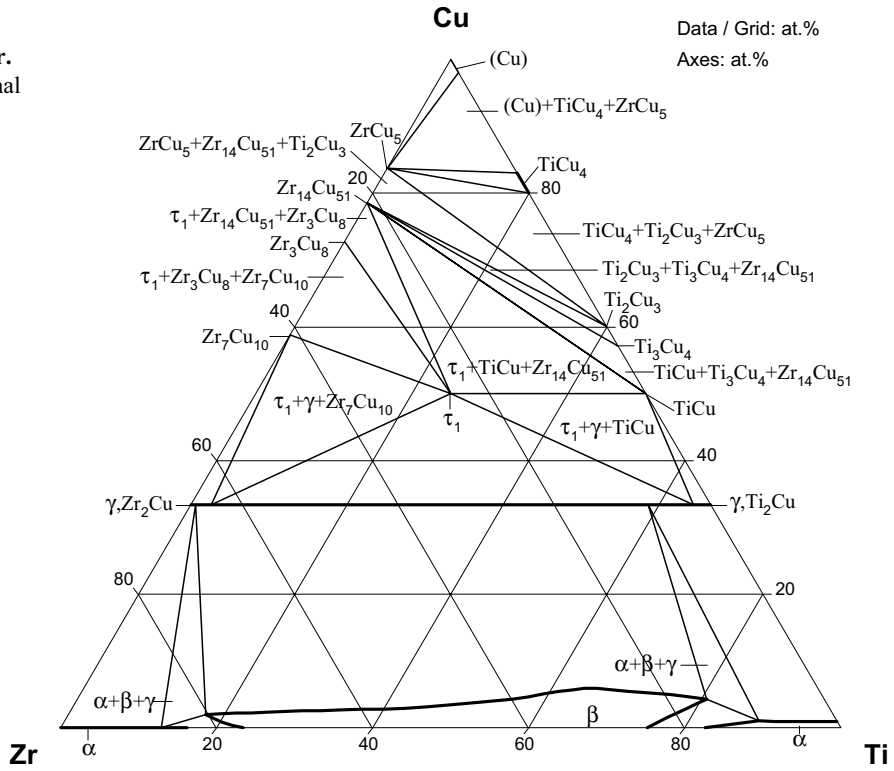

Fig. 14: Cu-Ti-Zr. Calculated isothermal section at 703°C

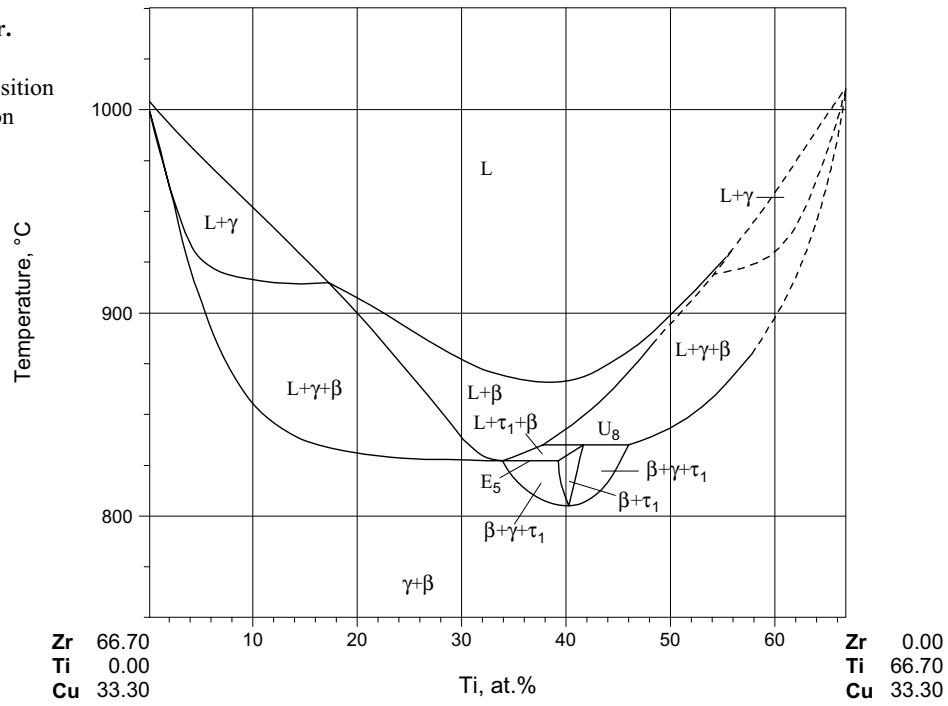

Fig. 15: Cu-Ti-Zr. Calculated temperature-composition Zr_2Cu-Ti_2Cu section

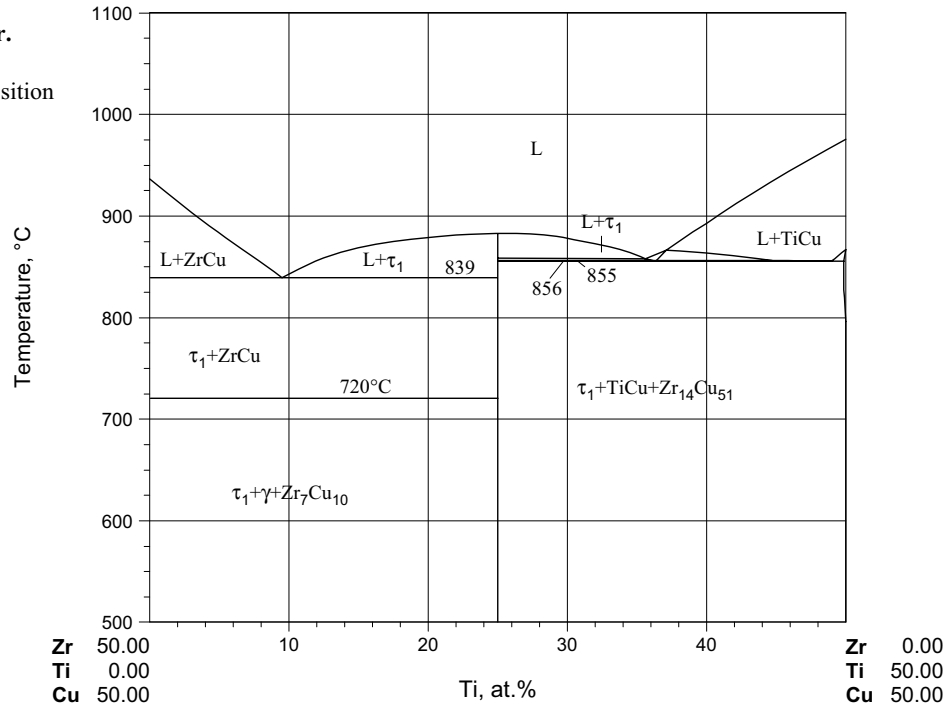

Fig. 16: Cu-Ti-Zr. Calculated temperature-composition ZrCu-TiCu section

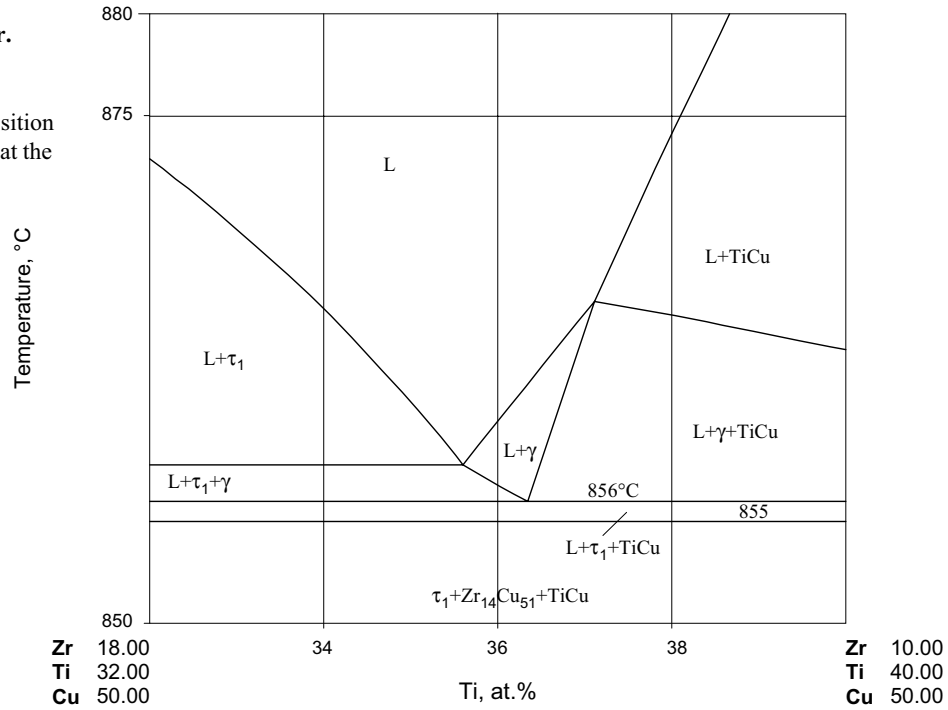

Fig. 17: Cu-Ti-Zr. Enlarged part of calculated temperature-composition ZrCu-TiCu section at the Ti composition 32 - 40 at.%

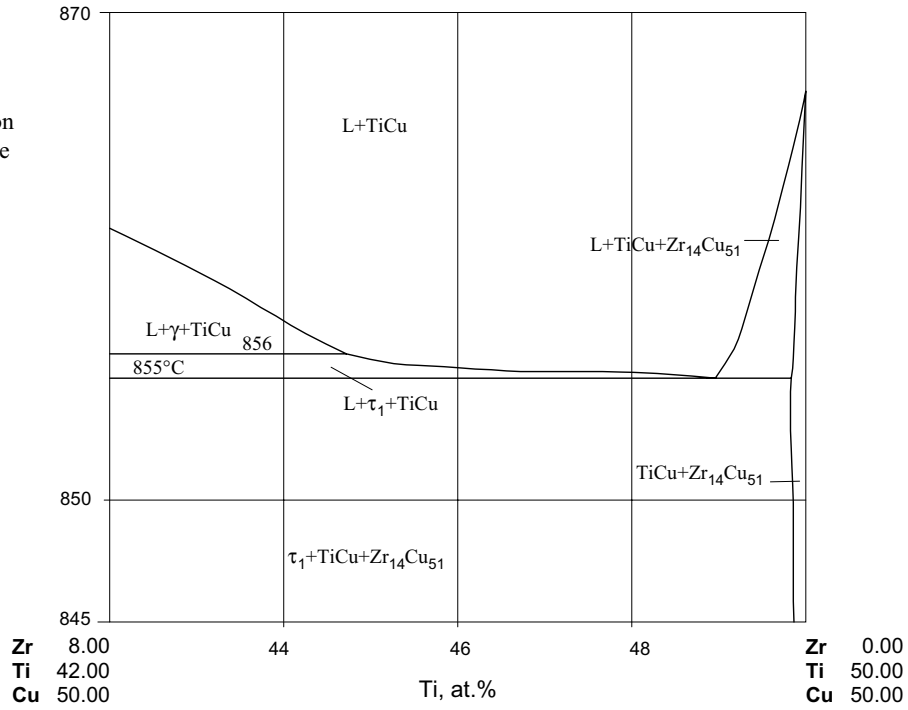

Fig. 19: Cu-Ti-Zr. Glass forming range in Cu-Ti-Zr alloys

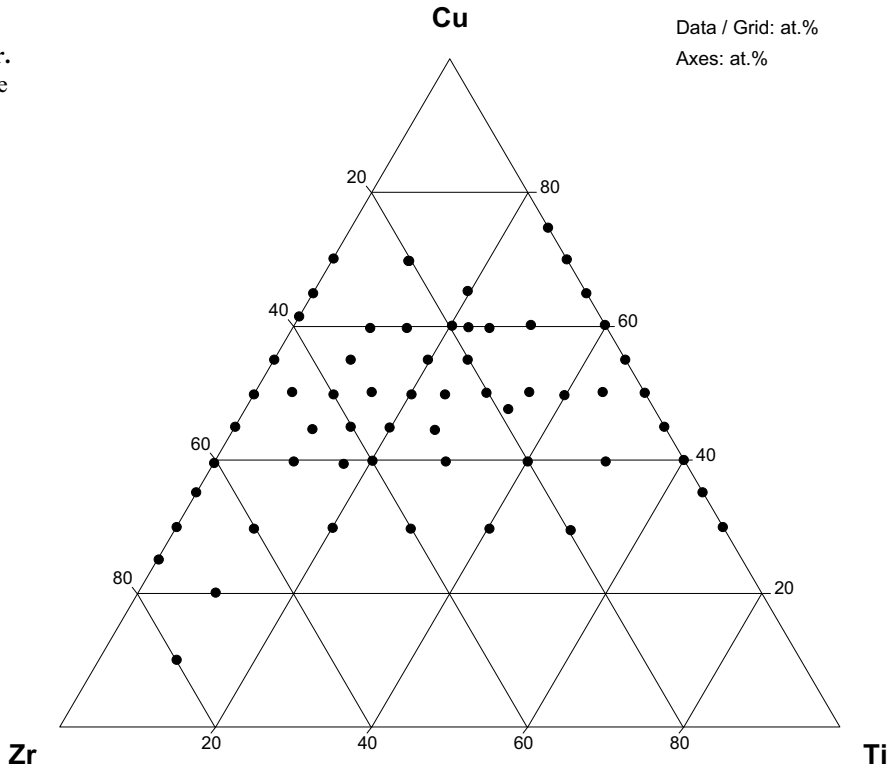

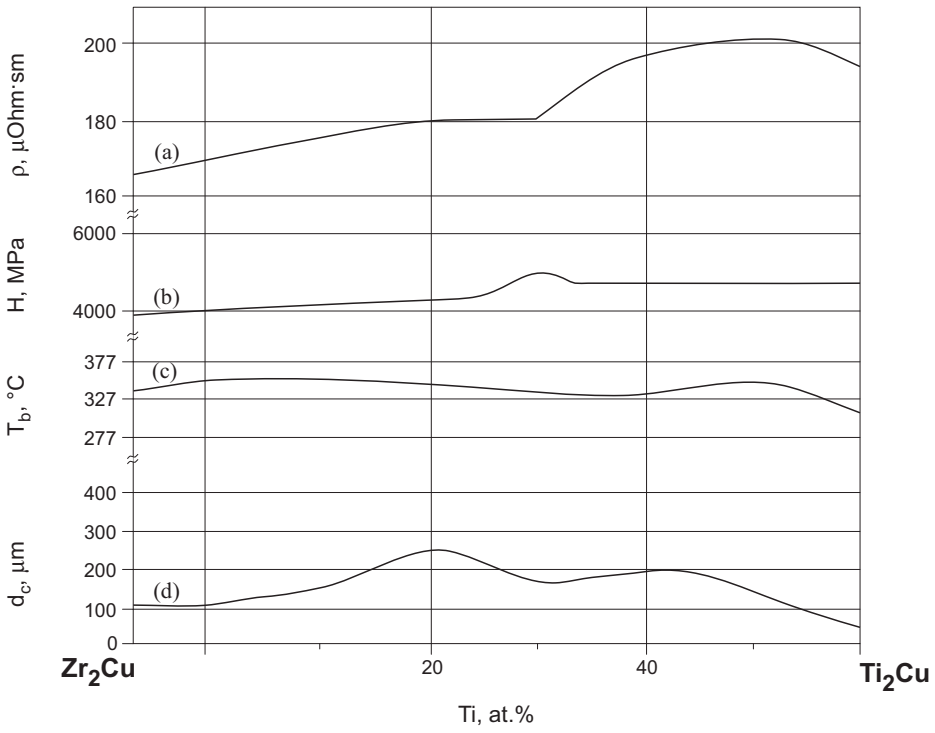

Fig. 20: Cu-Ti-Zr. Variation of properties of amorphous alloys with composition along the Zr_2Cu-Ti_2Cu section: a - electroresistance; b - microhardness; c - embrittlement temperature; d - critical thickness of amorphous alloys.

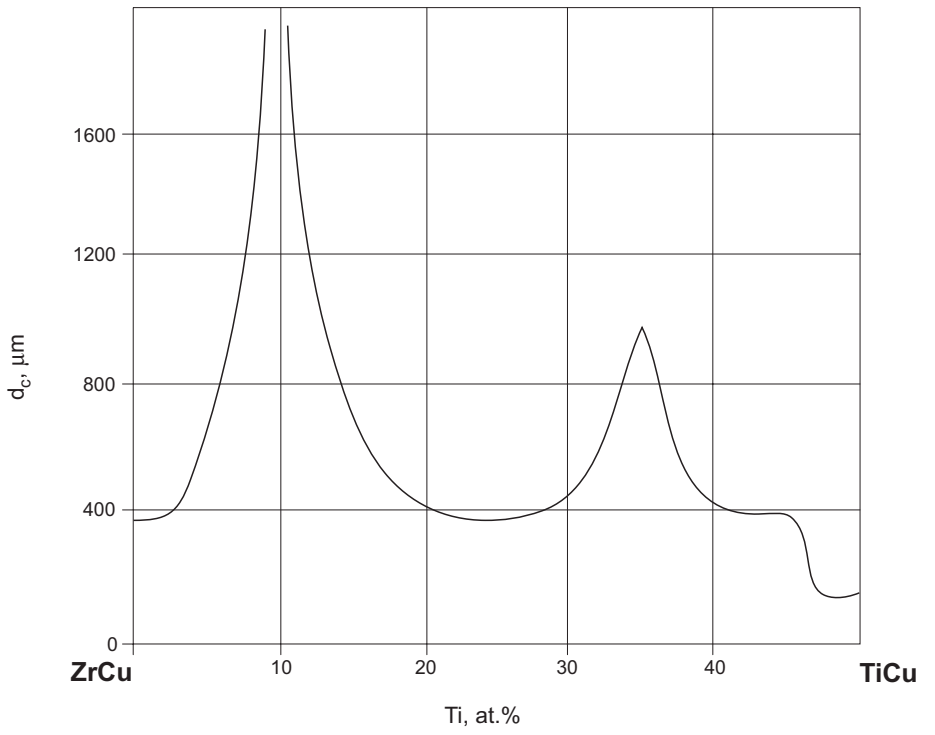

Fig. 21: Cu-Ti-Zr. Concentration dependence of critical thickness of amorphous alloys along the ZrCu-TiCu section

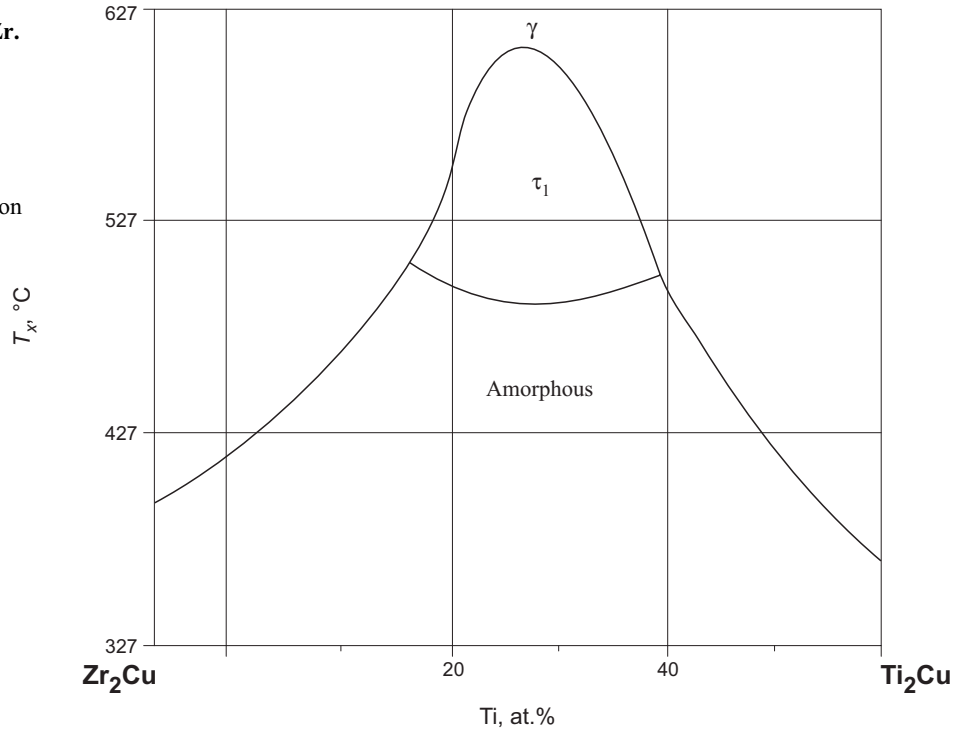

Fig. 22: Cu-Ti-Zr. Diagram of metastable crystallization of amorphous alloys along the Zr_2Cu-Ti_2Cu section